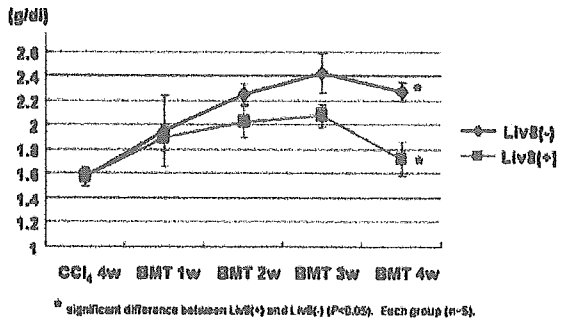


Fig. 6. The level of serum albumin. Serum albumin levels after Liv8-positive or Liv8-negative cell transplantation. $CCl_4$ 4w, 4 weeks $CCl_4$ injection group. BMT 1w, 1 week after BMC transplantation. BMT 2w, 2 weeks after BMC transplantation. BMT 3w, 3 weeks after BMC transplantation. BMT 4w, 4 weeks after BMC transplantation. * showed significant differences at each sampling point ($n = 5$) at $p < 0.05$.

liver at E11.5, but could not detect no-positive cells in fetal liver of AML1 knockout mice (Fig. 1C) at E 11.5. This result suggested that anti-Liv8-positive cell might be associated with the generation of HSC. We used FACS analysis to understand more about the characterization of Liv8-positive cells in the bone marrow. Around 32% of all BMCs, which were positive for Liv8, also expressed CD45 (Figs. 2A and B). CD45 is the pantrophic marker for hematopoietic cell marker [26,27]. These results suggest that anti-Liv8 recognizes most hematopoietic cells. We separated BMCs into Liv8-positive cells and Liv8-negative cells using AutoMACS, and the repopulation and transdifferentiation of these cells into liver was analyzed in the GFP/$CCl_4$ model [14].

First we analyzed the colonization of transplanted Liv8-positive or negative cell. There was no change in the ratio of GFP-positive cells one week after transplantation between the Liv8-positive and Liv8-negative cell groups (Figs. 3A and B). In both groups, GFP-positive cells were found around the portal vein. The expression of GFP decreased with time for the Liv8-positive cell group (Fig. 3C), but in the Liv8-negative cell group, GFP-positive cells entered the hepatic lobes (Fig. 3D). At four weeks after transplantation, the rate of colonization for the Liv8-positive cell group was significantly lower than that for the Liv8-negative cell group (Table 1). Previously we found that colonization was not observed when BMCs were transplanted to normal recipients, but colonization was observed when BMCs were transplanted to recipients with liver cirrhosis caused by administration of $CCl_4$ [14]. Some previous studies also have reported that $CCl_4$ injection enhances the repopulation of hepatocytes following hepatocyte transplantation via the spleen [28,29]. It has been documented that elevated levels of SDF1 and matrix metalloprotease 9 (MMP9) might have an important role for the migration of BMCs to the liver at liver damage by $CCl_4$ administration [16,30]. In the GFP/$CCl_4$, the expression of MMP9 was also increased by the transplantation of BMCs (I. Sakaida, unpublished data). At 1 week after transplantation, there was no marked difference in colonization between the Liv8-positive and negative transplantation groups. These results suggest that the early migration of BMC into liver was determined by the recipient condition. Next we analyzed the transdifferentiation of BMC into functional hepatocyte in the "niche" where transdifferentiation of BMC into hepatocyte is favorable [14]. The results of our past analyses have shown that transplanted BMCs transdifferentiate into Liv2-positive hepatoblasts and then differentiate into hepatocytes only under continuous inflammation. The persistent liver damage made by injection of persistent $CCl^4$ injection is important for the transdifferentiation of BMC [14]. When human HSCs were transplanted to immunologically tolerant NOD/SCID mice and followed up with administration of $CCl_4$, it was found that transplanted human HSC was differentiated into albumin express hepatocyte-like cell [15]. Albumin/promoter-Alb-DsRed2 Tg rat was established to monitor the transdifferentiation into albumin positive cell. Albumin-producing DsReds cell was increased by repeated administration of $CCl_4$ [31]. A study reported recently that the transdifferentiation of BMCs was low when inducing liver damage by $CCl_4$ administration before or after transplantation [32]. Different results were obtained with these systems because chronic liver damage before and after transplantation was not evident. The persistent liver damage might be the key factor to induce the transdifferentiation of BMC into hepatocyte. We investigated the transdifferentiation of Liv8 positive and negative BMCs into hepatoblast and hepatocytes by Liv2 and albumin expression. Like GFP, Liv2-positive cells were seen around the portal vein one week after transplantation for both Liv8-positive and Liv8-negative cell groups, and there was no marked difference between the two groups (Figs. 4A and B). On the other hand, at four weeks after transplantation, the expression of Liv2 for the Liv8-positive cell group was significantly lower than that for the Liv8-negative cell group (Figs. 4C and D). The results of double staining at four weeks after transplantation also showed that the number of myelogenic Liv2-positive cells was greater for the Liv8-negative cell group (Figs. 4E and F). Figs. 5C and D show the expression of albumin four weeks after transplantation and the expression of albumin for the Liv8-negative cell group was higher (Fig. 5D). The expression of albumin and GFP in myelogenic cells was significantly higher for the Liv8-negative cell group (Fig. 5F). Furthermore, we investigated functional recovery by comparing improvement in hepatic failure between the Liv8-positive and Liv8-negative cell groups.

As shown in Fig. 6, when $CCl_4$ was administered in the same manner to the Liv8-positive and Liv8-negative cell groups, and the level of serum albumin increased in both groups, but a significant finding in this analysis was significant improvements in the serum albumin levels at four weeks after transplantation in the Liv8-negative cell group compared to the Liv8-positive cell group ($p < 0.05$). These findings support those of immunostaining. These results can be summarized that Liv8-negative cells are more likely to transdifferentiate into hepatocytes with time passed. The subpopulation which was deleted by anti-Liv8 will be useful cells to use cell therapy using BMC to repair damaged liver. The Liv8 negative cell was thought to be non-hematopoietic cells. For example, multi-potent adult progenitor cells (MAPCs) from BMCs differentiate into functional hepatocyte like cells [33,34]. Our results might support that mesenchymal cells may differentiate into pluripotent cells under certain conditions.

Still the precise mechanisms to regulate repopulation and transdifferentiation BMC into hepatocyte are uncertain. To develop a cell therapy using BMC to repair damaged liver, we are planning to further analyze these mechanisms.

## Acknowledgments

We thank Dr. Masaru Okabe (Genome Research Center, Osaka University) for the gift of GFP transgenic mice and Mr. Jun Oba for his excellent support for immunohistochemistry.

## References

[1] B.E. Petersen, W.C. Bowen, K.D. Patrene, W.M. Mars, A.K. Sullivan, N. Murase, S.S. Boggs, et al., Bone marrow as a potential source of hepatic oval cells, Science 284 (1999) 1168–1170.
[2] N.D. Theise, M. Nimmakayalu, R. Gardner, P.B. Illei, G. Morgan, L. Teperman, O. Henegariu, et al., Liver from bone marrow in humans, Hepatology 32 (2000) 11–16.
[3] M.R. Alison, R. Poulsom, R. Jeffery, A.P. Dhillon, A. Quaglia, J. Jacob, M. Novelli, et al., Hepatocytes from non-hepatic adult stem cells, Nature 406 (2000) 257.
[4] D.S. Krause, N.D. Theise, M.I. Collector, O. Henegariu, S. Hwang, R. Gardner, S. Neutzel, et al., Multi-organ, multi-lineage engraftment by a single bone marrow-derived stem cell, Cell 105 (2001) 369–377.
[5] R. Okamoto, T. Yajima, M. Yamazaki, T. Kanai, M. Mukai, S. Okamoto, Y. Ikeda, et al., Damaged epithelia regenerated by bone marrow-derived cells in the human gastrointestinal tract, Nat. Med. 8 (2002) 1011–1017.
[6] M. Korbling, R.L. Katz, A. Khanna, A.C. Ruifrok, G. Rondon, M. Albitar, R.E. Champlin, et al., Hepatocytes and epithelial cells of donor origin in recipients of peripheral-blood stem cells, N. Engl. J. Med. 346 (2002) 738–746.
[7] S. Terai, N. Yamaoto, K. Omori, I. Sakaida, O. Kollet, A new cell therapy using bone marrow cells to repair damaged liver, J. Gastroenterol. 37 (Suppl. XIV) (2002) 162–163.
[8] A.J. Wagers, R.I. Sherwood, J.L. Christensen, I.L. Weissman, Little evidence for developmental plasticity of adult hematopoietic stem cells, Science 297 (2002) 2256–2259.
[9] E.L. Herzog, L. Chai, D.S. Krause, Plasticity of marrow-derived stem cells, Blood 102 (2003) 3483–3493.
[10] E. Lagasse, H. Connors, M. Al-Dhalimy, M. Reitsma, M. Dohse, L. Osborne, X. Wang, et al., Purified hematopoietic stem cells can differentiate into hepatocytes in vivo, Nat. Med. 6 (2000) 1229–1234.
[11] G. Vassilopoulos, P.R. Wang, D.W. Russell, Transplanted bone marrow regenerates liver by cell fusion, Nature 422 (2003) 901–904.
[12] X. Wang, H. Willenbring, Y. Akkari, Y. Torimaru, M. Foster, M. Al-Dhalimy, E. Lagasse, et al., Cell fusion is the principal source of bone-marrow-derived hepatocytes, Nature 422 (2003) 897–901.
[13] M. Okabe, M. Ikawa, K. Kominami, T. Nakanishi, Y. Nishimune, 'Green mice' as a source of ubiquitous green cells, FEBS Lett. 407 (1997) 313–319.
[14] S. Terai, I. Sakaida, N. Yamamoto, K. Omori, T. Wratanabe, S. Ohata, T. Katada, et al., An in vivo model for monitoring the transdifferentiation of bone marrow cells into functional hepatocytes, J. Biochem. (Tokyo) 134 (2003) 551–558.
[15] X. Wang, S. Ge, G. McNamara, Q.L. Hao, G.M. Crooks, J.A. Nolta, Albumin-expressing hepatocyte-like cells develop in the livers of immune-deficient mice that received transplants of highly purified human hematopoietic stem cells, Blood 101 (2003) 4201–4208.
[16] O. Kollet, S. Shivtiel, Y.Q. Chen, J. Suriawinata, S.N. Thung, M.D. Dabeva, J. Kahn, et al., HGF, SDF-1, and MMP-9 are involved in stress-induced human CD34+ stem cell recruitment to the liver, J. Clin. Invest. 112 (2003) 160–169.
[17] T. Kinoshita, A. Miyajima, Cytokine regulation of liver development, Biochim. Biophys. Acta 1592 (2002) 303–312.
[18] J. Wineman, K. Moore, I. Lemischka, C. Muller-Sieburg, Functional heterogeneity of the hematopoietic microenvironment: rare stromal elements maintain long-term repopulating stem cells, Blood 87 (1996) 4082–4090.
[19] M. Nanno, M. Hata, H. Doi, S. Satomi, H. Yagi, T. Sakata, R. Suzuki, et al., Stimulation of in vitro hematopoiesis by a murine fetal hepatocyte clone through cell–cell contact, J. Cell Physiol. 160 (1994) 445–454.
[20] H. Taniguchi, T. Toyoshima, K. Fukao, H. Nakauchi, Presence of hematopoietic stem cells in the adult liver, Nat. Med. 2 (1996) 198–203.
[21] T. Watanabe, K. Nakagawa, S. Ohata, D. Kitagawa, G. Nishitai, J. Seo, S. Tanemura, et al., SEK1/MKK4-mediated SAPK/JNK signaling participates in embryonic hepatoblast proliferation via a pathway different from NF-kappaB-induced anti-apoptosis, Dev. Biol. 250 (2002) 332–347.
[22] N. Uchida, T. Fujisaki, A.C. Eaves, C.J. Eaves, Transplantable hematopoietic stem cells in human fetal liver have a CD34(+) side population (SP) phenotype, J. Clin. Invest. 108 (2001) 1071–1077.
[23] M.F. Pittenger, A.M. Mackay, S.C. Beck, R.K. Jaiswal, R. Douglas, J.D. Mosca, M.A. Moorman, et al., Multilineage potential of adult human mesenchymal stem cells, Science 284 (1999) 143–147.
[24] T. Okuda, J. van Deursen, S.W. Hiebert, G. Grosveld, J.R. Downing, AML1, the target of multiple chromosomal translocations in human leukemia, is essential for normal fetal liver hematopoiesis, Cell 84 (1996) 321–330.
[25] K. Shinoda, S. Mori, T. Ohtsuki, Y. Osawa, An aromatase-associated cytoplasmic inclusion, the "stigmoid body," in the rat brain: I. Distribution in the forebrain, J. Comp. Neurol. 322 (1992) 360–376.
[26] H.K. Mikkola, Y. Fujiwara, T.M. Schlaeger, D. Traver, S.H. Orkin, Expression of CD41 marks the initiation of definitive hematopoiesis in the mouse embryo, Blood 101 (2003) 508–516.

[27] G.G. Wulf, K.L. Luo, M.A. Goodell, M.K. Brenner, Anti-CD45-mediated cytoreduction to facilitate allogeneic stem cell transplantation, Blood 101 (2003) 2434–2439.
[28] D. Guo, T. Fu, J.A. Nelson, R.A. Superina, H.E. Soriano, Liver repopulation after cell transplantation in mice treated with retrorsine and carbon tetrachloride, Transplantation 73 (2002) 1818–1824.
[29] S. Gupta, P. Rajvanshi, E. Aragona, C.D. Lee, P.R. Yerneni, R.D. Burk, Transplanted hepatocytes proliferate differently after $CCl_4$ treatment and hepatocyte growth factor infusion, Am. J. Physiol. 276 (1999) G629–G638.
[30] H.M. Hatch, D. Zheng, M.L. Jorgensen, B.E. Petersen, SDF-1alpha/CXCR4: a mechanism for hepatic oval cell activation and bone marrow stem cell recruitment to the injured liver of rats, Cloning Stem Cells 4 (2002) 339–351.
[31] Y. Sato, Y. Igarashi, Y. Hakamata, T. Murakami, T. Kaneko, M. Takahashi, et al., Establishment of Alb-DsRed2 transgenic rat for liver regeneration research, Biochem. Biophys. Res. Commun. 311 (2) (2003) 478–481.
[32] Y. Kanazawa, I.M. Verma, Little evidence of bone marrow-derived hepatocytes in the replacement of injured liver, Proc. Natl. Acad. Sci. USA 100 (Suppl. 1) (2003) 11850–11853.
[33] R.E. Schwartz, M. Reyes, L. Koodie, Y. Jiang, M. Blackstad, T. Lund, T. Lenvik, et al., Multipotent adult progenitor cells from bone marrow differentiate into functional hepatocyte-like cells, J. Clin. Invest. 109 (2002) 1291–1302.
[34] Y. Jiang, B.N. Jahagirdar, R.L. Reinhardt, R.E. Schwartz, C.D. Keene, X.R. Ortiz-Gonzalez, M. Reyes, et al., Pluripotency of mesenchymal stem cells derived from adult marrow, Nature 418 (2002) 41–49.

*J. Biochem.* **134**, 551–558 (2003)
DOI: 10.1093/jb/mvg173

# An *In Vivo* Model for Monitoring *Trans*-Differentiation of Bone Marrow Cells into Functional Hepatocytes

**Shuji Terai*[,1], Isao Sakaida[1], Naoki Yamamoto[1], Kaoru Omori[1], Tomomi Watanabe[2], Shinya Ohata[2], Toshiaki Katada[2], Koji Miyamoto[3], Koh Shinoda[4], Hiroshi Nishina[3] and Kiwamu Okita[1]**

[1]*Department of Molecular Science & Applied Medicine (Gastroenterology & Hepatology), Yamaguchi University School of Medicine, Minami Kogushi 1-1-1, Ube, Yamaguchi 755-8505;* [2]*Department of Physiological Chemistry, Graduate School of Pharmaceutical Sciences, University of Tokyo, Tokyo 113-0033;* [3]*Department of Molecular Science & Applied Medicine (Bio-Regulation), Yamaguchi University School of Medicine, Minami Kogushi 1-1-1, Ube, Yamaguchi 755-8505; and* [4]*Departmemt of Neuro-anatomy & Neuroscience, Yamaguchi University School of Medicine, Minami Kogushi 1-1-1, Ube, Yamaguchi 755-8505*

Received June 24, 2003; accepted July 28, 2003

**The plasticity of bone marrow cells (BMCs) remains controversial. The present study found that persistent injury induces efficient trans-differentiation of BMCs into functional hepatocytes. Mice with liver cirrhosis induced by carbon tetrachloride were injected with $1 \times 10^5$ non-treated green fluorescent protein (GFP)-positive BMCs via the tail vein. In these mice, transplanted GFP-positive BMCs efficiently migrated into the peri-portal area of liver lobules after one day, repopulating 25% of the recipient liver by 4 weeks. In contrast, no GFP-positive BMCs were detected following transplantation into control mice with undamaged livers. BMCs trans-differentiated into functional mature hepatocytes via immature hepatoblasts. Serum albumin levels were significantly elevated to compensate for chronic liver failure in BMC transplantation. These results reveal that recipient conditions and microenvironments represent key factors for successful cell therapy using BMCs.**

**Key words: bone marrow cell, hepatic stem cell, niche, oval cell, *trans*-differentiation.**

Abbreviations: BMC, bone marrow cell; $CCl_4$, carbon tetrachloride; EGFP, enhanced GFP; ES cell, embryonic stem cell; FAH, fumarylacetoacetate hydrolase; GFP, green fluorescent protein; HNF4, hepatocyte nuclear factor 4; MAPCs, multipotent adult progenitor cells; NGS, normal goat serum; NRS, normal rabbit serum; PAP, peroxidase-antiperoxidase.

The use of stem cells in regenerative medicine is attractive as a potential approach to curing patients with severe disease. Embryonic stem (ES) cells are pluripotent cells that differentiate into numerous cell types *in vivo* and *in vitro* (*1*). Although ES cells can be isolated from humans, ethical considerations and problems with the production of teratoma complicate their use in human therapies. Conversely, adult stem cells exist in various tissues (*2–7*). The use of tissue-specific stem cells is attractive, but isolating these cells can sometimes prove difficult, and their capacity for self-renewal is limited. Several groups have recently reported the capacity of bone marrow cells (BMCs) to differentiate into various non-hematopoietic cell lineages (*8–12*). These results suggest BMCs as an attractive cell source for regenerative medicine, as the cells are more easily obtained than other tissue-specific stem cells (*13*). The capacity of BMCs to differentiate into hepatocytes and intestinal cells has been demonstrated using Y chromosome detection in autopsy analyses of human female recipients of BMCs from male donors (*9*, *14*, *15*). However, following reports that spontaneous cell fusion is an important mechanism for trans-differentiation of BMCs and tissue stem cells, many researchers cannot accept the existence of adult BMCs that display a multipotent capacity for differentiation (*16*, *17*). Lagasse *et al.* reported that purified hematopoietic stem cells differentiated into hepatocytes in a fumarylacetoacetate hydrolase (FAH)-deficient model (*12*). Wang and Vassllopoulos *et al.* recently reported that cell fusion is an important mechanism for explaining the differentiation of BMCs into hepatocytes in the FAH-deficient model (*18*, *19*). Conversely, other groups have reported finding no evidence of cell fusion during trans-differentiation of BMCs into pancreatic endocrine cells and buccal epithelial cells in vivo (*20*, *21*). Newsome *et al.* reported that human umbilical cord blood-derived cells can differentiate into hepatocytes in mouse liver without evidence of cell fusion (*22*). Jiang *et al.* established multipotent adult progenitor cells (MAPCs) in bone marrow using a culturing system derived from mesenchymal stem cells (*23*, *24*). The plasticity and trans-differentiation of BMCs thus remain controversial. To develop effective cell therapies using BMCs, a better understanding of the regulatory mechanisms controlling BMC plasticity and differentiation into non-hematopoietic cell lineages is required. To address these issues, we developed a new *in vivo* model to monitor the differentiation of BMCs into functional hepatocytes. In this model, BMCs are transplanted without prior culture. The development of this new model should greatly advance our understanding of

*To whom correspondence should be addressed. Tel: +81-836-22-2241, Fax: +81-836-22-2240, E-mail: terais@yamaguchi-u.ac.jp

BMC plasticity. We selected a liver cirrhosis model in mice subjected to injections of carbon tetrachloride ($CCl_4$) for 4 weeks, due to its similarities to liver cirrhosis in humans. This study used transgenic mice expressing Green Fluorescence Protein (GFP) as a source of BMCs to explore the process of BMC differentiation into hepatocytes (*25*). GFP-positive BMCs were isolated and transplanted into liver cirrhosis mice without the addition of culture step. If BMC transplantation successfully compensates for liver failure, new cell therapies for patients with chronic liver damage can be developed. This model was also used to analyze the differentiation process of BMCs into hepatocytes.

## MATERIAL AND METHODS

*Mice*—C57BL6/Tg14 (act-EGFP) OsbY01 mice were kindly provided by Masaru Okabe (Genome Research Center, Osaka University, Osaka). All tissues from the transgenic mice appeared green under excitation light (*25*). Female C57BL/6 mice were purchased from Japan SLC (Shizuoka). Mice were properly anesthetized during experiments. All procedures including surgical steps were performed in accordance with Yamaguchi University guidelines for experiments involving animals and recombinant DNA.

*BMC Preparation and Transplantation*—For the isolation of BMCs, C57BL6/Tg 14 (act-EGFP) OsbY01 mice (6-weeks-old) were killed by cervical dislocation, and their limbs were removed. GFP-positive BMCs were flushed from the medullary cavities of the tibias and femurs using a 25G needle and Dulbecco's modified Eagle's culture medium with 10% fetal bovine serum. Marrow cell preparation took approximately 1.5 h.

In the liver damage group, 0.5 ml/kg of $CCl_4$ was injected into the peritoneum of 6-weeks-old C57BL/6 females twice a week for 4 weeks. Liver cirrhosis resulting from the continuous injections of $CCl_4$ was confirmed. One day after the eighth injection, $1 \times 10^5$ GFP-positive BMCs were injected slowly into the tail vein using a 31G needle and a Hamilton syringe. After transplantation, $CCl_4$ injections were continued at the same dose twice a week. As a control, $1 \times 10^5$ GFP-positive BMCs were injected into female C57BL/6 mice that had not been treated with $CCl_4$.

*Tissue Preparation*—The livers were thoroughly perfused *via* the heart with 4% paraformaldehyde (Muto, Tokyo). This step was crucial for washing out contaminating blood cells. For fixation, the perfused livers were incubated with 4% paraformaldehyde (Muto) overnight, then soaked in 30% sucrose for a few more 3 days. Tissues were frozen in dry ice and then sectioned into 18-μm slices using a cryostat (Moriyasu Kounetsu, Osaka) in preparation for dyeing.

*Immunohistochemistry and Double Immunofluorescence for GFP*—Cells expressing GFP were analyzed by both fluorescent microscopy and conventional immunohistochemistry with anti-GFP antibody (Santa Cruz Biotechnology, Santa Cruz, California, USA). Immunohistochemical analysis was performed in accordance with previously reported methods (*26*). Tissues were soaked overnight in 0.3% Triton X-100/0.05% normal goat serum (NGS; Chemicon, Temecula, CA, USA) or normal rabbit serum (NRS; Chemicon) and phosphate-buffered saline (PBS). The next day, the tissues were immersed in 500 μl of 10% NGS or NRS/0.3% TritonX-100/PBS for 3 h, then washed with 0.3% Triton X-100/PBS/0.05% NGS or NRS for 10 min. Tissues were soaked in 1.5% $H_2O_2$/50% methanol/DDW for 2 h, then washed with 0.3% Triton X-100/PBS/0.05% NGS or NRS. Sections were incubated overnight with anti-GFP antibody (1:5,000 FL, sc-8334; Santa Cruz Biotechnology), anti–HNF-4 (1:5000 H-171; Santa Cruz Biotechnology), anti-albumin (1:5,000, 55462; ICN Pharmaceuticals, Costa Mesa, CA, USA), anti-Liv2 antibody (1:5,000) (*27*) or A6 monoclonal antibody (1:5,000) for common surface-exposed antigens of mouse on oval cells and biliary epithelial cells (*28*). Tissues were then washed three times for 10 minutes each with 0.3% Triton X-100/PBS/0.05% NGS or NRS. Tissues were incubated with biotin-conjugated IgG anti-rat, -rabbit, -mouse, -goat IgG (Dako, Kyoto) as secondary antibodies for 2 h at 37°C, then washed three times for 20 min each with PBS. After incubation with both peroxidase-antiperoxidase (PAP)-goat, mouse, rabbit (Dako), PAP-rat IgG complex (Chemicon) and streptavidin (Dako) as the third antibody for 3 h at 37°C, the tissues were washed with 0.05 M Tris-HCl buffer (pH 7.4). Samples were then treated with 0.05 M Tris-HCl buffer (pH 7.4) containing 0.02% diaminobenzine and 0.6% nickel ammnonium sulfate (DAB-nickel solution) in the presence of 0.005% $H_2O_2$ (nickel-enhanced DAB reaction) for 10–15 min at room temperature. For fluorescence immunohistochemistry, tissues were incubated with Alexa Fluor R 488 and 568 donkey anti-goat IgG(H+L) conjugate, Alexa Fluor R 488 goat anti-rabbit IgG(H+L) conjugate and Alexa Fluor R 568 goat anti-rat IgG(H+L) conjugate (Molecular Probes, Eugene, OR) as secondary antibodies for 3 h, then washed with PBS. Sections were mounted on glass slides in 1% gelatin/saline. Positive cells in the liver were quantified using a Provis microscope (Olympus, Tokyo) equipped with a charge coupled devise (CCD) camera, and subjected to computer-assisted image analysis with MetaMorph software (Universal Imaging Corporation, Downingtown, PA). A total of 10 different areas per liver section were analyzed independently, and the areas of positive cells were calculated using the MetaMorph software.

*Serum Albumin Levels*—Serum albumin levels were measured in experimental mice for 4 weeks after BMC transplantation and in control mice using a SPOTCHEM EZ SP-4430 dry chemical system (Arkray, Kyoto).

*Statistical Analysis*—Values are shown as mean ± SE. Data were analyzed by analysis of variance with Fisher's projected least significant difference test.

## RESULTS

*GFP Positive BMCs Migrated into the Peri-Portal Region of Liver Lobules then Distributed into Lobules with Chronic Liver Damage*—We injected $1 \times 10^5$ GFP-positive BMCs into both liver-damaged and control (undamaged) mice. After transplantation, $CCl_4$ treatment at the same dose was continued twice each week. Transplanted cells were visualized immunohistochemically using anti-GFP antibody (Fig. 1, a–f). No GFP-positive cells were detected in liver sections of undamaged

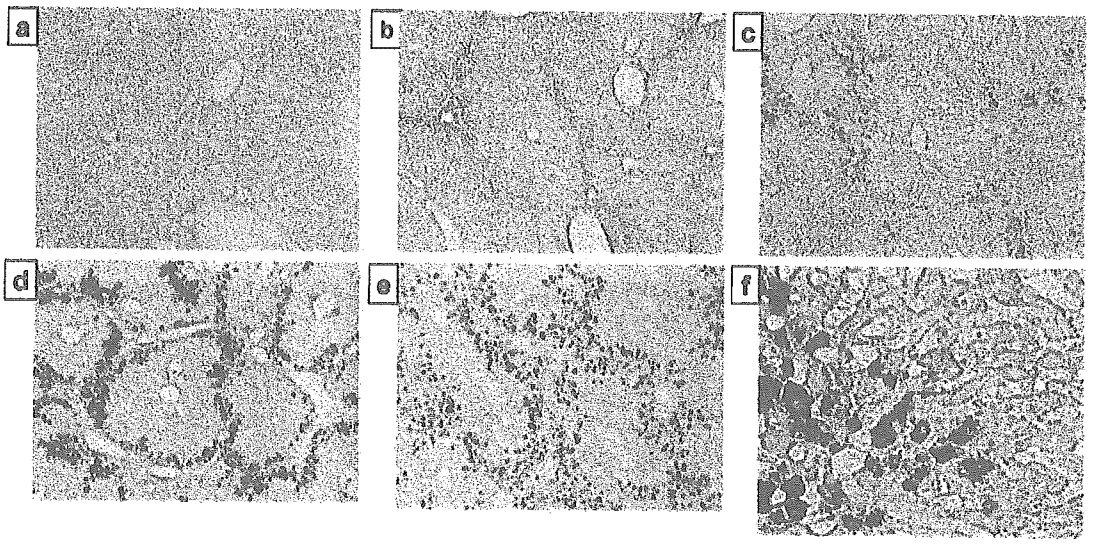


Fig. 1. **Expression of GFP.** a: Anti-GFP staining of a liver section 1 week after BMC transplantation in the control group (no $CCl_4$ treatment). Magnification ×200. b: Anti-GFP staining of a liver section after 4 weeks of $CCl_4$-induced liver damage without BMC transplantation. Magnification ×200. c–f: Liver sections of BMC transplant recipients in the $CCl_4$-induced liver damage group. Magnification ×200. The brown color of the liver sections resulted from a pH difference in the detection buffer, but sensitivity was unaffected. c: 1 d after BMC transplantation. d: 1 week after transplantation. e: 4 weeks. f: Higher magnification at 4 weeks, ×400.

controls (Fig. 1a) or in mice with $CCl_4$ damage but no BMC transplantation (Fig. 1b). In contrast, the edges of peri-portal regions of liver lobules from BMC recipients treated with $CCl_4$ contained 0.1–1% GFP-positive BMCs one day after BMC transplantation (Fig. 1c). The number of GFP-positive cells gradually increased, spreading into the liver lobules 1–4 weeks after transplantation (Fig. 1, d and e) and forming liver cell cords (Fig. 1f). The areas occupied by GFP-positive cells increased each week up to 26 ± 1% at 4 weeks (Table 1). These results indicate that GFP-positive BMCs migrate into the peri-portal areas of damaged liver and proliferate to form hepatic cords at 4 weeks only under conditions of persistent liver damage.

*BMCs Differentiated into Hepatocytes Expressing Different Differentiation Markers*—To monitor the differentiation of transplanted BMCs into hepatocytes, cells were tested for the concommitant expression of GFP and various differentiation markers: hepatoblast markers Liv2; hepatocyte nuclear factor 4 (HNF4) (*29–32*), and hepatocyte marker albumin. Liv2 represents a marker for hepatoblasts in the hepatic bud (*27*). Liv2-positive cells were not detected in bone marrow (data not shown) or in persistently damaged livers without BMC transplantation (Fig. 2a). Liv2-positive cells appeared in the peri-portal regions of the liver 1 week after BMC transplantation (Fig. 2b), and then increased and spread throughout the liver lobules (Fig. 2, b and c). Liv2-positive cells occupied up to 21 ± 1% of affected lobules (Table 1) and were detected at liver cell cords at 4 weeks (Fig. 2d). The co-expression of Liv2 and GFP (yellow color cell) is shown in Fig. 2 (e and f).

HNF4 expression was also analyzed. HNF4 is a transcription factor associated with hepatocyte differentiation (*29–32*). In the livers of BMC-recipient mice, HNF4 expression and HNF4-occupied areas increased over time (Fig. 3, a and b, and Table 1). Co-expression of HNF4 and GFP is shown in Fig. 3c. Staining with an A6 oval cell-specific monoclonal antibody (*28*) detected positive cells in the peri-portal region 1 week after BMC transplantation (Fig. 3d). The area occupied by A6-positive cells was about 5–6% by 4 weeks after BMC transplantaion (Fig. 3e and Table 1). However, A6-positive cells that also expressed GFP were not found in liver after BMC transplantation (data not shown). A6-positive cells were not detected in $CCl_4$-damaged livers without BMC transplantation (Fig. 3f) or in normal livers (Fig. 3g).

Table 1. **Areas occupied by various differentiation markers after BMC transplantation into the persistent liver damage group.**

| | 1 week ($n = 4$) | 2 weeks ($n = 4$) | 3 weeks ($n = 4$) | 4 weeks ($n = 4$) |
|---|---|---|---|---|
| GFP | 12 ± 1 | 15 ± 1 | 21 ± 2*,** | 26 ± 1*,**,*** |
| Liv2 | 11 ± 1 | 14 ± 1* | 18 ± 1*,** | 21 ± 1*,**,*** |
| HNF4 | 16 ± 1 | 19 ± 1* | 16 ± 1** | 20 ± 1*,*** |
| A6 | 5 ± 1 | 6 ± 1 | 6 ± 1 | 6 ± 1 |
| Albumin | 9 ± 2 | 12 ± 2 | 27 ± 1*,** | 42 ± 1*,**,*** |

Value are shown as mean ± SE. *Significant difference compared with the value at 1 week ($p < 0.05$). **Significant difference compared with the value at 2 weeks ($p < 0.05$). ***Significant difference compared with the value at 3 weeks ($p < 0.05$) ($n = 4$).

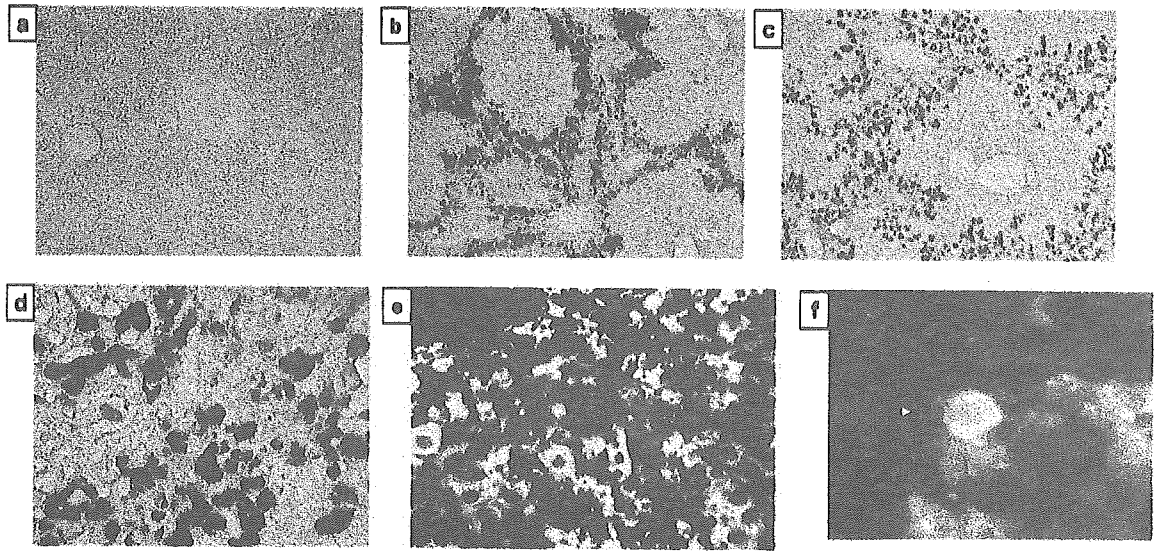


Fig. 2. **Expression of Liv2 antigen.** Immunohistochemistry of liver sections from $CCl_4$-treated mice. a: Absence of Liv2-positive cells after 4 weeks of $CCl_4$ treatment in mice without BMC transplantation. Magnification ×200. b, c: Liv2 expression at (b) 1 week and (c) 4 weeks after BMC transplantation. Magnification ×200. d: Magnified image at 4 weeks, ×400. e: Double fluorescent images (red, Liv2; green, GFP; yellow, Liv2 and GFP) at 4 weeks. A GFP-positive cell expressing Liv2 appears yellow, ×400. f: Higher magnification of the cell co-expressing GFP and Liv2, ×400.

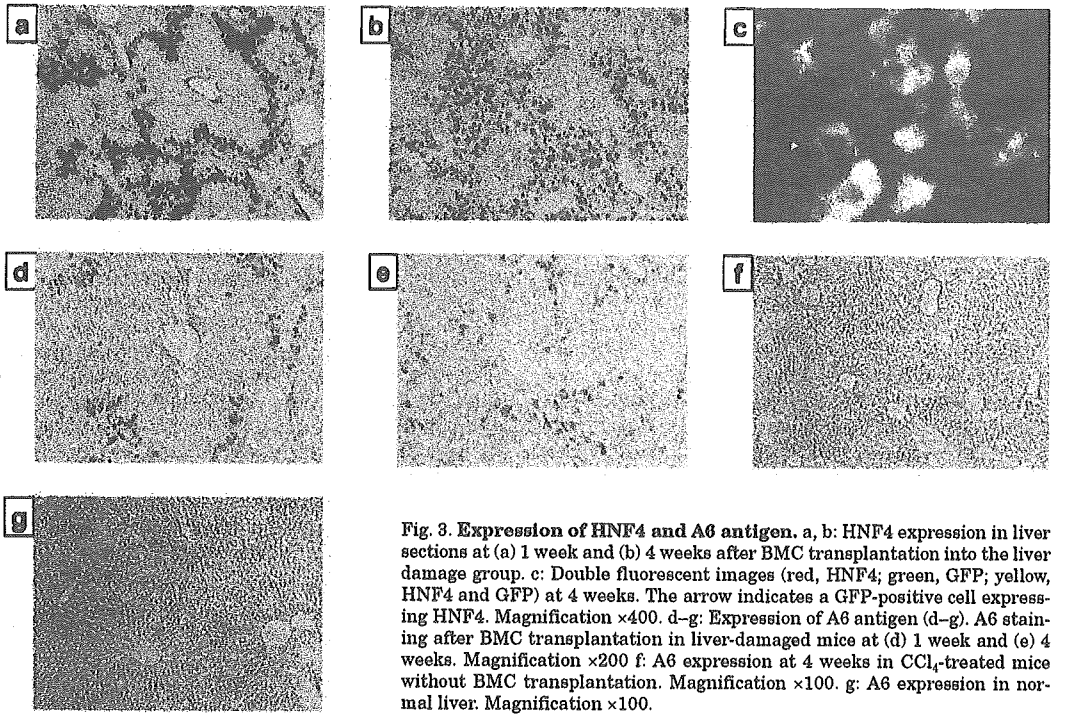


Fig. 3. **Expression of HNF4 and A6 antigen.** a, b: HNF4 expression in liver sections at (a) 1 week and (b) 4 weeks after BMC transplantation into the liver damage group. c: Double fluorescent images (red, HNF4; green, GFP; yellow, HNF4 and GFP) at 4 weeks. The arrow indicates a GFP-positive cell expressing HNF4. Magnification ×400. d–g: Expression of A6 antigen (d–g). A6 staining after BMC transplantation in liver-damaged mice at (d) 1 week and (e) 4 weeks. Magnification ×200 f: A6 expression at 4 weeks in $CCl_4$-treated mice without BMC transplantation. Magnification ×100. g: A6 expression in normal liver. Magnification ×100.

*BMCs Differentiate into Functionally Mature Hepatocytes and Compensate for Chromic Liver Failure Induced by Persistent Liver Damage*—Whether transplanted BMCs can differentiate into functional hepatocytes was evaluated by analyzing albumin expression. Albumin was detected as dark staining in hepatocytes of normal mouse liver sections (Fig. 4a). The expression of albumin decreased in the livers of mice treated with $CCl_4$ for 4 weeks without

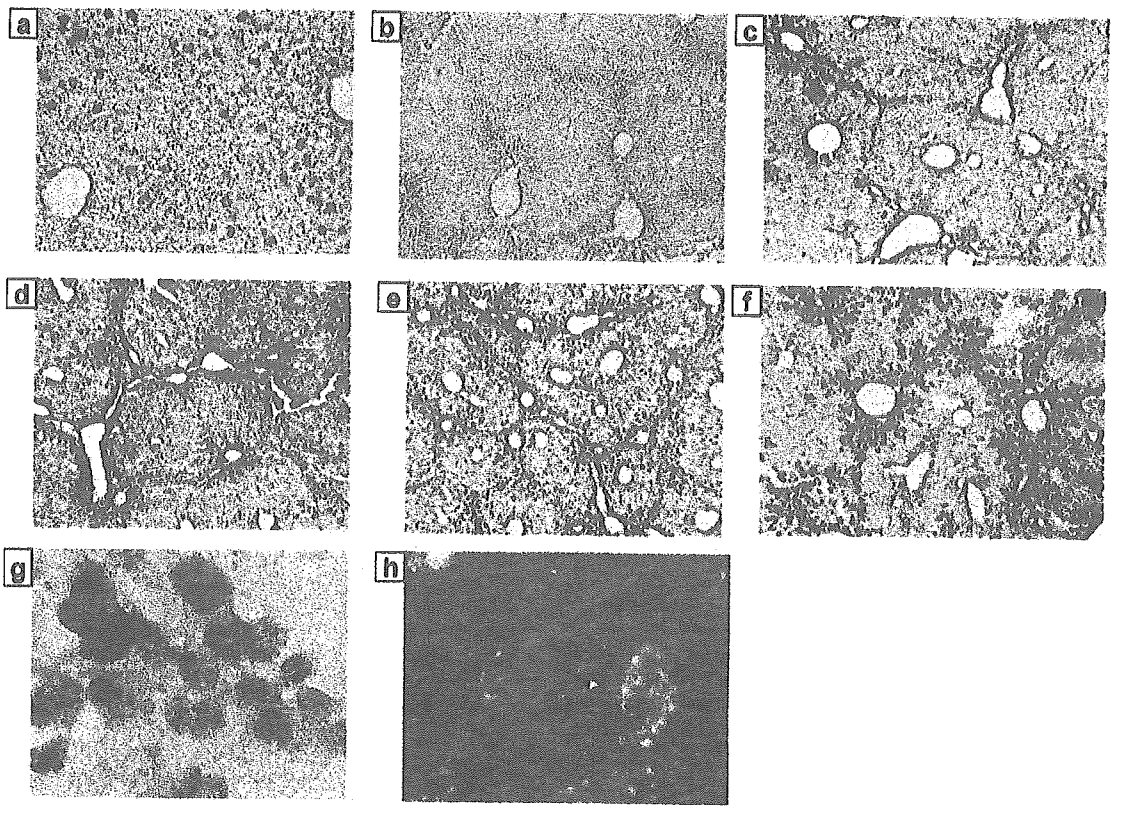


Fig. 4. **Albumin expression.** a: Albumin expression in a liver section from a normal mouse. Magnification ×200. b: Liver section of a mouse after 4 weeks of $CCl_4$ treatement. Magnification ×200. c–f: Albumin expression after BMC transplantation in the liver damage group at (c) 1 week, (d) 2 weeks, (e) 3 weeks, and (f) 4 weeks. Magnification ×200. g: Higher magnification at 4 weeks. h: Double fluorescent image (red, albumin; green, GFP; yellow, albumin and GFP) at 4 weeks after BMC transplantation in the liver damage group. Magnification ×400. The arrow indicates the co-expression of albumin and GFP in one cell.

BMC transplantation (Fig. 4b). At 1 week after BMC transplantation, a small number of albumin-positive cells were apparent in the peri-portal regions of damaged livers (Fig. 4c). The mean area occupied by albumin-positive cells was 9 ± 2% at 1 week (Table 1). Cells expressing high levels of albumin increased in number and spread from the peri-portal regions into lobules over time (Fig. 4, c–f, and Table 1). Cells expressing high levels of albumin were also detected in liver cell cords (Fig. 4g). Co-expression of GFP (green) and albumin (red) was observed; the albumin in co-expressing cells appeared as fine yellow particles (Fig. 4h). Areas displaying albumin increased to 42 ± 1% at 4 weeks, although the GFP-occupied areas comprised only 26 ± 1% (Table 1). To determine whether BMC transplantation compensates for liver damage, serum albumin levels were analyzed in the persistent liver damage groups with and without BMC transplantation (Fig. 5). The serum albumin level of $CCl_4$-damaged mice not undergoing BMC transplantation decreased over time, to 1.62 ± 0.15 g/dl at 8 weeks ($n = 5$). In contrast, the serum albumin levels in $CCl_4$-damaged mice subjected to BMC transplantation increased to 2.08 ± 0.10 g/dl by 4 weeks after BMC transplantation, representing a significant difference ($p < 0.05$). These results demonstrate that transplanted BMCs differentiate into functional hepatocytes that can compensate for liver damage.

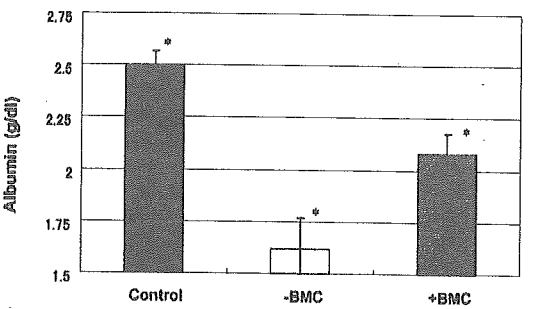


Fig. 5. **Serum albumin levels of $CCl_4$-treated mice with or without BMC transplantation.** Control, normal mice. Values indicate albumin levels of normal control mice. -BMC, $CCl_4$-treated mice without BMC transplantation. Values show albumin levels after 8 weeks $CCl_4$ injection without BMC transplantaion. +BMC, $CCl_4$-treated mice who underwent BMC transplantation. Values show albumin levels of recipient mice at 4 weeks after BMC transplantation. *Differences between groups were significant ($n = 5$; $p < 0.05$).

## DISCUSSION

The present study described a new *in vivo* model for monitorng the *trans*-differentiation of BMCs into hepatocytes using GFP as a marker protein. In these experiments, the areas occupied by GFP-positive cells comprised around 0.1–1% by 1 day after BMC transplantaion (Fig. 1c). Transplanted GFP-positive BMCs migrated into the peri-portal regions of cirrhotic livers (Fig. 1d). Gangandeep *et al.* reported that hepatocytes transplanted *via* the spleen distributed to the peri-portal region immediately in dipeptidyl peptidase IV–deficient F344 rats with $CCl_4$-induced cirrhosis (*33*). Although the BMCs in our model were transplanted *via* the tail vein, the same efficient migration of transplanted cells to the peri-portal regions of cirrhotic livers occurred. The areas of liver occupied by GFP-positive cells increased to 26 ± 1% by 4 weeks after BMC transplantation, despite continued induction of liver damage by the injection of $CCl_4$ (Table 1). Some previous studies have reported that $CCl_4$ injection enhances the repopulation of hepatocytes following hepatocyte tranplantation *via* the spleen (*34*, *35*). The same situation might have occurred in the present model. In FAH-deficient mice, transplanted hematopoietic stem cells were found to form foci of hematopoietic stem cell-derived hepatocytes to compensate for liver failure (*12*). Conversely, in our experiments, transplanted GFP-positive BMCs formed hepatic cords in the liver in a different manner (Fig. 1f), representing a major difference between the FAH model and this $CCl_4$ model.

Recently, cell fusion has been reported as an important mechanism for the plasticity of BMCs and tissue stem cells (*16*, *17*). The differentiation of BMCs into hepatocytes in the FAH model seems to indicate cell fusion as an important mechanism of differentiation (*18*, *19*). However, other groups have reported finding no evidence of cell fusion during the *trans*-differentiation of BMCs into other cell lineages *in vivo* (*20*, *21*). We analyzed the rate of cell fusion using cultured Neo-resistant ES cells and GFP-positive BMCs under the same culture conditions as Terada *et al.* (*17*), who reported a cell fusion rate of $1/10^5$–$10^6$. Our in vitro assay yielded similar results (data not shown). Next we analyzed the differentiation step from transplanted BMC into hepatocyte. To monitor the differentiation of transplanted BMCs into hepatocytes, the expressions of hepatoblast markers Liv2 (*27*), HNF4, and hepatocyte marker albumin, and the hepatic oval cell marker A6 were analyzed. During mouse liver development, Liv2-positive cells appear in the hepatic bud at E 9.5 d. In our study, Liv2-positive cells were not detected in bone marrow (data not shown) or in persistently damaged liver without BMC transplantation (Fig. 2a). Liv2-positive cells appeared in the peri-portal regions of the liver 1 week after BMC transplantation and had spread throughout the damaged liver lobules (Fig. 2, b–d), to occupy 21 ± 1% of liver area at 4 weeks (Table 1). Liv2-expressing cells were also detected in liver cell cords at 4 week (Fig. 2d). The co-expression of Liv2 and GFP (yellow colored cells) is shown in Fig. 2 (e and f), but cells co-expressing Liv2 and albumin were not observed (data not shown). These results suggest that transplanted BMCs change to an immature phenotype that expresses Liv2 antigen before maturing into albumin-expressing hepatocytes. HNF4 is a transcription factor associated with hepatocyte differentiation (*29–32*). In the livers of BMC-recipient mice, HNF4 expression and the HNF4-occupied area increased over time (Fig. 3, a and b, and Table 1). The co-expression of HNF4 and GFP is shown in Fig. 3c. These results suggest that differentiating BMCs take on the hepatocyte phenotype. Oval cells are considered to represent a type of hepatic stem cell derived from the Canal of Hering following severe liver damage (*6*, *37*). Petersen et al. also reported that under certain conditions, oval cells can be derived from BMCs (*8*). Therefore, the activation of oval cells was also analyzed using an A6 antibody. A6-positive cells were detected in the peri-portal regions 1 week after BMC transplantation (Fig. 3d). The A6-positive oval cells were activated, but the area occupied by A6-positive cells remained at around 5% even after 4 weeks (Fig. 3, d and e, and Table 1). However, A6-positive cells also expressing GFP were not detected in liver following BMC transplantation (data not shown). Furthermore, A6-positive cells were not detected in $CCl_4$-damaged livers without BMC transplantation (Fig. 3f), or in normal livers (Fig. 3g). These results suggest that while some signals activating oval cells are induced by BMC transplantation, oval cells might not be derived from transplanted BMCs. Although the possibility of cell fusion occurring in our model can not be excluded, BMCs were found to *trans*-differentiate into Liv2-positive hepatoblasts that subsequently differentiated into functional hepatocytes. The differentiation process resembles that observed during hepatogenesis (*38*).

Finally, we analyzed whether transplanted BMCs could differentiate into functional hepatocytes by examining albumin expression. Albumin was detected as a dark staining of hepatocytes in normal mouse liver sections (Fig. 4a), and its expression was decreased by persistent liver damage (Fig. 4b). At 1 week after BMC transplantation, a small number of albumin-positive cells appeared in the peri-portal regions of damaged livers (Fig. 4c), with the mean area occupied by albumin-positive cells being 9 ± 2% at 1 week (Table 1). Cells expressing high levels of albumin increased in number and spread from the peri-portal regions into damaged lobules over time (Fig. 4, c–f, and Table 1). Cells expressing high levels of albumin were also detected in liver cell cords (Fig. 4g). Co-expression of GFP (green) and albumin (red) was observed, with the albumin in co-expressing cells appearing as fine yellow particles (Fig. 4h). The area occupied by albumin-expressing cells increased to 42 ± 1% at 4 weeks, compared with the GFP-occupied area of only 26 ± 1% (Table 1). During the *trans*-differentiation of BMCs into hepatocytes, A6-positive oval cells are activated (Fig. 3, d and e and Table 1). These results suggest that the *trans*-differentiation of BMCs might affect albumin expression in surrounding cells *via* oval cell activation. Serum albumin levels decreased in persistent $CCl_4$-damaged mice without BMC transplantation, but increased significantly in $CCl_4$-damaged mice who underwent BMC transplantation at 4 weeks after transplantation (Fig. 5). These results demonstrate that transplanted BMCs differentiate into functional hepatocytes that can compensate for chronic liver failure.

Previously, several authors have reported the existence of hepatic stem/progenitor cells in bone marrow (*8*, *12*,

*39*). Jiang *et al.* derived MAPCs from bone marrow mesenchymal cells (*23, 24*) and engrafted $1.0 \times 10^6$ MAPCs into NOD/SCID mice. The MAPCs were found to occupy 5–8% of the liver area after 4–24 weeks. While the MAPCs demonstrated multipotency, their efficiency of differentiation into hepatocytes was lower than that observed in the present system, in which $1 \times 10^5$ BMC efficiently differentiated and occupied $26 \pm 1\%$ of the liver area by 4 weeks after transplantation. A significant increase in serum albumin levels demonstrated that the BMC-derived cells restored liver function. Exactly why the BMCs in our model were able to differentiate efficiently into functional hepatocytes remains an intriguing question. Only isolated BMCs were transplanted in the present system, without the addition of a culture period, representing one key difference from the methods described by Jiang *et al.* (*24*). Although exactly which cells trans-differentiate into hepatocytes remains unknown, we believe that the persistent liver damage induced by $CCl_4$ represents a key factor in our method, creating a special "differentiation niche" able to induce the trans-differentiation of BMCs into functional hepatocytes. Stress-induced signaling pathways are known to play crucial roles in hepatogenesis, and knockout mice for various inflammation signal molecules display massive liver degeneration (*40–42*). Based on these results, we postulate that the *trans*-differentiation of BMCs might be enhanced by unknown signals related to stress and inflammation.

In conclusion, much about the trans-differentiation of transplanted BMCs into hepatocytes in our model remains yet to be explained. However, our model shows that recipient condition and the timing of BMC transplantation are important. This system should facilitate the development of cell therapies for liver damage by providing a model for testing factors critical to BMC differentiation into hepatocytes.

This study was supported by grants-in-aid for Scientific Research from the Japan Society for the Promotion of Science (No. 13470121 to Shuji Terai, Isao Sakaida and Kiwamu Okita; and No. 13770262 to Shuji Terai) and for translational research from the Ministry of Health, Labor and Welfare (H-trans-5 to Shuji Terai, Isao Sakaida, Hiroshi Nishina and Kiwamu Okita). We wish to thank Dr. Snorri Thorgeirsson (Laboratory of Experimental Carcinogenesis, National Cancer Institute, NIH) for critical feedback on this manuscript. We are grateful to Dr. Masaru Okabe (Genome Research Center, Osaka University) for the donation of GFP transgenic mice, and to Mr. Jun Oba for valuable technical support with the immunohistochemistry. We also wish to thank Dr. Valentina Factor for providing us with the A6 antibody.

## REFERENCES

1. Thomson, J.A. and Odorico, J.S. (2000) Human embryonic stem cell and embryonic germ cell lines. *Trends Biotechnol.* **18**, 53–57
2. Weissman, I.L. (2000) Translating stem and progenitor cell biology to the clinic: barriers and opportunities. *Science* **287**, 1442–1446
3. Gage, F.H. (2000) Mammalian neural stem cells. *Science* **287**, 1433–1438
4. Potten, C.S. (1998) Stem cells in gastrointestinal epithelium: numbers, characteristics and death. *Philos. Trans. R. Soc. Lond. B. Biol. Sci.* **353**, 821–830
5. Moles, J.P. and Watt, F.M. (1997) The epidermal stem cell compartment: variation in expression levels of E-cadherin and catenins within the basal layer of human epidermis. *J. Histochem. Cytochem.* **45**, 867–874
6. Grisham, J.W. and Thorgeirsson, S.S. (1997) Liver stem cells in Stem Cell (Potten, C.S., ed.) pp. 233–282, Academic Press, Manchester
7. Pittenger, M.F., Mackay, A.M., Beck, S.C., Jaiswal, R.K., Douglas, R., Mosca, J.D., Moorman, M.A., Simonetti, D.W., Craig, S., and Marshak, D.R. (1999) Multilineage potential of adult human mesenchymal stem cells. *Science* **284**, 143–147
8. Petersen, B.E., Bowen, W.C., Patrene, K.D., Mars, W.M., Sullivan, A.K., Murase, N., Boggs, S.S., Greenberger, J.S., and Goff, J.P. (1999) Bone marrow as a potential source of hepatic oval cells. *Science* **284**, 1168–1170
9. Theise, N.D., Nimmakayalu, M., Gardner, R., Illei, P.B., Morgan, G., Teperman, L., Henegariù, O., and Krause, D.S. (2000) Liver from bone marrow in humans. *Hepatology* **32**, 11–16
10. Alison, M.R., Poulsom, R., Jeffery, R., Dhillon, A.P., Quaglia, A., Jacob, J., Novelli, M., Prentice, G., Williamson, J., and Wright, N.A. (2000) Hepatocytes from non-hepatic adult stem cells. *Nature* **406**, 257
11. Krause, D.S., Theise, N.D., Collector, M.I., Henegariu, O., Hwang, S., Gardner, R., Neutzel, S., and Sharkis, S.J. (2001) Multi-organ, multi-lineage engraftment by a single bone marrow-derived stem cell. *Cell* **105**, 369–377
12. Lagasse, E., Connors, H., Al-Dhalimy, M., Reitsma, M., Dohse, M., Osborne, L., Wang, X., Finegold, M., Weissman, I.L., and Grompe, M. (2000) Purified hematopoietic stem cells can differentiate into hepatocytes *in vivo*. *Nat. Med.* **6**, 1229–1234
13. Orlic, D., Kajstura, J., Chimenti, S., Jakoniuk, I., Anderson, S.M., Li, B., Pickel, J., McKay, R., Nadal-Ginard, B., Bodine, D.M., Leri, A., and Anversa, P. (2001) Bone marrow cells regenerate infarcted myocardium. *Nature* **410**, 701–705
14. Korbling, M., Katz, R.L., Khanna, A., Ruifrok, A.C., Rondon, G., Albitar, M., Champlin, R.E., and Estrov, Z. (2002) Hepatocytes and epithelial cells of donor origin in recipients of peripheral-blood stem cells. *N. Engl. J. Med.* **346**, 738–746
15. Okamoto, R., Yajima, T., Yamazaki, M., Kanai, T., Mukai, M., Okamoto, S., Ikeda, Y., Hibi, T., Inazawa, J., and Watanabe, M. (2002) Damaged epithelia regenerated by bone marrow-derived cells in the human gastrointestinal tract. *Nat. Med.* **8**, 1011–1017
16. Ying, Q.L., Nichols, J., Evans, E.P., and Smith, A.G. (2002) Changing potency by spontaneous fusion. *Nature* **416**, 545–548
17. Terada, N., Hamazaki, T., Oka, M., Hoki, M., Mastalerz, D.M., Nakano, Y., Meyer, E.M., Morel, L., Petersen, B.E., and Scott, E.W. (2002) Bone marrow cells adopt the phenotype of other cells by spontaneous cell fusion. *Nature* **416**, 542–545
18. Wang, X., Willenbring, H., Akkari, Y., Torimaru, Y., Foster, M., Al-Dhalimy, M., Lagasse, E., Finegold, M., Olson, S., and Grompe, M. (2003) Cell fusion is the principal source of bone-marrow-derived hepatocytes. *Nature* **422**, 897–901
19. Vassilopoulos, G., Wang, P.R., and Russell, D.W. (2003) Transplanted bone marrow regenerates liver by cell fusion. *Nature* **422**, 901–904
20. Ianus, A., Holz, G.G., Theise, N.D., and Hussain, M.A. (2003) In vivo derivation of glucose-competent pancreatic endocrine cells from bone marrow without evidence of cell fusion. *J. Clin. Invest.* **111**, 843–850
21. Tran, S.D., Pillemer, S.R., Dutra, A., Barrett, A.J., Brownstein, M.J., Key, S., Pak, E., Leakan, R.A., Kingman, A., Yamada, K.M., Baum, B.J., and Mezey, E. (2003) Differentiation of human bone marrow-derived cells into buccal epithelial cells *in vivo*: a molecular analytical study. *Lancet* **361**, 1084–1088
22. Newsome, P.N., Johannessen, I., Boyle, S., Dalakas, E., Mcaulay, A.K., Samuel, K., Rae, F., Forrester, L., Turner, M.L., Hayes, P.C., Harrison, D.J., Bickmore, W.A., and Plevris, J.N. (2003) Human cord blood-derived cells can differentiate into

hepatocyte in the mouse liver with no evidence of cellular fusion. *Gastroenterology* **124**, 1891–1900
23. Schwartz, R.E., Reyes, M., Koodie, L., Jiang, Y., Blackstad, M., Lund, T., Lenvik, T., Johnson, S., Hu, W.S., and Verfaillie, C.M. (2002) Multipotent adult progenitor cells from bone marrow differentiate into functional hepatocyte-like cells. *J. Clin. Invest.* **109**, 1291–1302
24. Jiang, Y., Jahagirdar, B.N., Reinhardt, R.L., Schwartz, R.E., Keene, C.D., Ortiz-Gonzalez, X.R., Reyes, M., Lenvik, T., Lund, T., Blackstad, M., Du, J., Aldrich, S., Lisberg, A., Low, W.C., Largaespada, D.A., and Verfaillie, C.M. (2002) Pluripotency of mesenchymal stem cells derived from adult marrow. *Nature* **418**, 41–49
25. Okabe, M., Ikawa, M., Kominami, K., Nakanishi, T., and Nishimune, Y. (1997) 'Green mice' as a source of ubiquitous green cells. *FEBS Lett.* **407**, 313–319
26. Shinoda, K., Mori, S., Ohtsuki, T., and Osawa, Y. (1992) An aromatase-associated cytoplasmic inclusion, the "stigmoid body," in the rat brain: I. Distribution in the forebrain. *J. Comp. Neurol.* **322**, 360–376
27. Watanabe, T., Nakagawa, K., Ohata, S., Kitagawa, D., Nishitai, G., Seo, J., Tanemura, S., Shimizu, N., Kishimoto, H., Wada, T., Aoki, J., Arai, H., Iwatsubo, T., Mochita, M., Satake, M., Ito, Y., Matsuyama, T., Mak, T., Penninger, J., Nishina, H., and Katada, T. (2002) SEK1/MKK4-Mediated SAPK/JNK Signaling Participates in Embryonic Hepatoblast Proliferation via a Pathway Different from NF-kappaB-Induced Anti-Apoptosis. *Dev. Biol.* **250**, 332–347
28. Factor, V.M., Radaeva, S.A., and Thorgeirsson, S.S. (1994) Origin and fate of oval cells in dipin-induced hepatocarcinogenesis in the mouse. *Amer. J. Pathol.* **145**, 409–422
29. Zaret, K. (1998) Early liver differentiation: genetic potentiation and multilevel growth control. *Curr. Opin. Genet. Dev. Dev.* **8**, 526–531
30. Nagy, P., Bisgaard, H.C., and Thorgeirsson, S.S. (1994) Expression of hepatic transcription factors during liver development and oval cell differentiation. *J. Cell Biol.* **126**, 223–233
31. Li, J., Ning, G., and Duncan, S.A. (2000) Mammalian hepatocyte differentiation requires the transcription factor HNF-4alpha. *Genes Dev.* **14**, 464–474
32. Kamiya, A., Inoue, Y., and Gonzalez, F.J. (2003) Role of the hepatocyte nuclear factor 4alpha in control of the pregnane X receptor during fetal liver development. *Hepatology* **37**, 1375–1384
33. Gagandeep, S., Rajvanshi, P., Sokhi, R.P., Slehria, S., Palestro, C.J., Bhargava, K.K., and Gupta, S. (2000) Transplanted hepatocytes engraft, survive, and proliferate in the liver of rats with carbon tetrachloride-induced cirrhosis. *J. Pathol.* **191**, 78–85
34. Gupta, S., Rajvanshi, P., Aragona, E., Lee, C.D., Yerneni, P.R., and Burk, R.D. (1999) Transplanted hepatocytes proliferate differently after CCl4 treatment and hepatocyte growth factor infusion. *Amer. J. Physiol.* **276**, G629–638
35. Guo, D., Fu, T., Nelson, J.A., Superina, R.A., and Soriano, H.E. (2002) Liver repopulation after cell transplantation in mice treated with retrorsine and carbon tetrachloride. *Transplantation* **73**, 1818–1824
36. Wang, X., Montini, E., Al-Dhalimy, M., Lagasse, E., Finegold, M., and Grompe, M. (2002) Kinetics of liver repopulation after bone marrow transplantation. *Amer. J. Pathol.* **161**, 565–574
37. Petersen, B.E., Zajac, V.F., and Michalopoulos, G.K. (1998) Hepatic oval cell activation in response to injury following chemically induced periportal or pericentral damage in rats. *Hepatology* **27**, 1030–1038
38. Shiojiri, N., Lemire, J.M., and Fausto, N. (1991) Cell lineages and oval cell progenitors in rat liver development. *Cancer Res.* **51**, 2611–2620
39. Theise, N.D., Badve, S., Saxena, R., Henegariu, O., Sell, S., Crawford, J.M., and Krause, D.S. (2000) Derivation of hepatocytes from bone marrow cells in mice after radiation-induced myeloablation. *Hepatology* **31**, 235–240
40. Beg, A.A., Sha, W.C., Bronson, R.T., Ghosh, S., and Baltimore, D. (1995) Embryonic lethality and liver degeneration in mice lacking the RelA component of NF-kappa B. *Nature* **376**, 167–170
41. Li, Q., Van Antwerp, D., Mercurio, F., Lee, K.F., and Verma, I.M. (1999) Severe liver degeneration in mice lacking the IkappaB kinase 2 gene. *Science* **284**, 321–325
42. Nishina, H., Vaz, C., Billia, P., Nghiem, M., Sasaki, T., de la Pompa, J.L., Furlonger, K., Paige, C., Hui, C., Fischer, K.D., Kishimoto, H., Iwatsubo, T., Katada, T., Woodgett, J.R., and Penninger, J.M. (1999) Defective liver formation and liver cell apoptosis in mice lacking the stress signaling kinase SEK1/MKK4. *Development* **126**, 505–516

# Dual Phosphorylation of Phosphoinositide 3-Kinase Adaptor Grb2-Associated Binder 2 Is Responsible for Superoxide Formation Synergistically Stimulated by Fcγ and Formyl-Methionyl-Leucyl-Phenylalanine Receptors in Differentiated THP-1 Cells[1]

Haruka Momose,[2] Hiroshi Kurosu,[2] Noriko Tsujimoto, Kenji Kontani, Kyoko Tsujita, Hiroshi Nishina, and Toshiaki Katada[3]

**The class Ia phosphoinositide (PI) 3-kinase consisting of p110 catalytic and p85 regulatory subunits is activated by Tyr kinase-linked membrane receptors such as FcγRII through the association of p85 with the phosphorylated receptors or adaptors. The heterodimeric PI 3-kinase is also activated by G protein-coupled chemotactic fMLP receptors, and activation of the lipid kinase plays an important role in various immune responses, including superoxide formation in neutrophils. Although fMLP-induced superoxide formation is markedly enhanced in FcγRII-primed neutrophils, the molecular mechanisms remain poorly characterized. In this study, we identified two Tyr-phosphorylated proteins, c-Cbl (Casitas B-lineage lymphoma) and Grb2-associated binder 2 (Gab2), as PI 3-kinase adaptors that are Tyr phosphorylated upon the stimulation of FcγRII in differentiated neutrophil-like THP-1 cells. Interestingly, Gab2 was, but c-Cbl was not, further Ser/Thr phosphorylated by fMLP. Thus, the adaptor Gab2 appeared to be dually phosphorylated at the Ser/Thr and Tyr residues through the two different types of membrane receptors. The Ser/Thr phosphorylation of Gab2 required the activation of extracellular signal-regulated kinase, and fMLP receptor stimulation indeed activated extracellular signal-regulated kinase in the cells. Enhanced superoxide formation in response to Fcγ and fMLP was markedly attenuated when the Gab2 Ser/Thr phosphorylation was inhibited. These results show the importance of the dual phosphorylation of PI 3-kinase adaptor Gab2 for the enhanced superoxide formation in neutrophil-type cells.** *The Journal of Immunology,* **2003, 171: 4227–4234.**

Neutrophils or polymorphonuclear leukocytes move and orientate themselves in gradients of chemotactic substances released from invading microorganisms. Stimulation of chemotactic receptors by formyl peptides such as fMLP induces neutrophil migration and other responses, including the generation of reactive oxygen species and the release of lysosomal enzymes, which are essential for host defense. At site of infection, FcγR, which recognize Fc portion of IgG, play an important role in host defense, together with the chemotactic receptor. Foreign organisms are covered with host IgG, and the extracellular immunocomplexes are rapidly phagocytized through Fcγ receptors and finally digested by fusion with intracellular lysosomes (see Refs. 1–3 for review).

We have previously reported that fMLP-induced superoxide formation was markedly enhanced by FcγRII cross-linking in differentiated THP-1 cells and that this response was completely abolished by treatment with wortmannin, a specific inhibitor of phosphoinositide (PI)[4] 3-kinase (4–6). Furthermore, accumulation of the PI 3-kinase product phosphatidylinositol 3, 4, 5-triphosphate ($PIP_3$) in response to fMLP is enhanced by the simultaneous stimulation of FcγRII. It is, therefore, conceivable that the activation of PI 3-kinase plays a crucial role in enhanced superoxide generation in neutrophil-type THP-1 cells.

PI 3-kinase catalyzes phosphorylation of inositol phospholipids at the 3-position of inositol ring. It can be classified into three groups (class I, II, and III) according to the structure and substrate specificity, and only the class I PI 3-kinase family can generate $PIP_3$. Furthermore, the class I PI 3-kinase is comprised of two types in terms of mode of activation in mammalian cells: one (class Ia) is stimulated by receptors linked to Tyr kinase (α, β, and δ types), and the other (class Ib) is activated by G protein-coupled receptors (γ type). The PI 3-kinase α, β, and δ are heterodimers consisting of a 110-kDa catalytic subunit (p110) and an 85-kDa regulatory subunit (p85); the p85 subunit possesses two Src homology 2 (SH2) domains. The interaction of Tyr-phosphorylated

Department of Physiological Chemistry, Graduate School of Pharmaceutical Sciences, University of Tokyo, Tokyo, Japan

Received for publication January 15, 2003. Accepted for publication August 14, 2003.

The costs of publication of this article were defrayed in part by the payment of page charges. This article must therefore be hereby marked *advertisement* in accordance with 18 U.S.C. Section 1734 solely to indicate this fact.

[1] This work was supported in part by research grants from the "Research for the Future" Program of the Japan Society for the Promotion of Science (JSPS-RFTF 96L00505), the Mitsubishi Foundation, and the Scientific Research Funds of the Ministry of Education, Culture, Sports, Science and Technology of the Japanese Government.

[2] H.M. and H.K. contributed equally to this work.

[3] Address correspondence and reprint requests to Dr. Toshiaki Katada, Department of Physiological Chemistry, Graduate School of Pharmaceutical Sciences, University of Tokyo, Tokyo 113-0033, Japan. E-mail address: katada@mol.f.u-tokyo.ac.jp

[4] Abbreviations used in this paper: PI, phosphoinositide; Cbl, Casitas B-lineage lymphoma; ERK, extracellular signal-regulated kinase; Gab2, Grb2-associated binder 2; MBP, myelin basic protein; $PIP_3$, phosphatidylinositol 3,4,5-triphosphate; PP2A, protein phosphatase 2A; SH2, Src homology 2.



0022-1767/03/$02.00

receptors or adaptors with the SH2 domains of p85 is a dominant step for activating the enzyme (see Refs. 7 and 8 for review).

We also reported that the class Ia PI 3-kinase consisting of p110β and p85 has unique properties in terms of the regulation of its lipid kinase activity (9, 10). The p110β/p85 isoform can be synergistically activated by a Tyr-phosphorylated peptide and the βγ subunits of G proteins. Such synergistic activation was, however, not observed in other class Ia PI 3-kinases (10). Thus, the p110β/p85 isoform appears to be responsible for the synergistic activation by two different types of membrane receptors, one possessing Tyr kinase activity and the other activating trimeric GTP-binding proteins (9). Subsequently, these unique properties observed in the p110β/p85 isoform were also confirmed by the study of Maier et al. (11). As described above, cellular responses stimulated by both Fcγ and fMLP receptors, such as enhanced superoxide formation, appear to be associated with the synergistic activation of p110β/p85 PI 3-kinase. However, the precise mechanisms underlying this priming process are presently unclear.

In this study, we examined the activation mechanism of p110β/p85 PI 3-kinase from the point of its associated molecules. We found that Grb2-associated binder 2 (Gab2) and c-Cbl (Casitas B-lineage lymphoma) function as Tyr-phosphorylated adaptors for PI 3-kinase in FcγRII-stimulated THP-1 cells and that the adaptor Gab2 is further phosphorylated on Ser/Thr residue(s) by extracellular signal-regulated kinase (ERK) upon the stimulation with fMLP. Interestingly, this dual phosphorylation on Gab2 appears to be responsible for the enhanced superoxide formation in neutrophil-like THP-1 cells.

## Materials and Methods

### *Materials*

Anti-p110β, anti-Cbl, and anti-ERK2 Abs were purchased from Santa Cruz Biotechnology (Santa Cruz, CA). Anti-p85 and anti-Gab2 (anti-Gab2/C) Abs were purchased from Seikagaku Kogyo (Tokyo, Japan) and Upstate Biotechnology (Lake Placid, NY), respectively. Another anti-Gab2 Ab (anti-Gab2/P) was obtained by immunizing rabbit with keyhole limpet hemocyanin-conjugated peptide (CVRQSSEPSKGAKL) corresponding to the C terminus of human Gab2. Anti-FcγRII (CD32) IV.3 (subclass IgG2b; 025-101) and $F(ab')_2$ of goat anti-mouse IgG (201-1806) were purchased from Medarex (Annandale, NJ) and Kirkegaard & Perry Laboratories (Gaithersburg, MD), respectively. An anti-phospho-Tyr Ab (AB1600) was obtained from Chemicon International (Temecula, CA). Sepharose 4B and protein A-Sepharose 4-FF were from Pharmacia Biotech (Uppsala, Sweden). PMA, fMLP, staurosporine, myelin basic protein (MBP), and protein phosphatase 2A (PP2A) were purchased from Sigma-Aldrich (St. Louis, MO). A mitogen-activated protein kinase kinase inhibitor, PD98059, was purchased from Calbiochem (San Diego, CA). [$\gamma$-$^{32}$P]ATP and $^{125}$I-labeled protein A were purchased from DuPont NEN (Boston, MA). HRP-labeled anti-rabbit IgG was from Jackson ImmunoResearch Laboratories (West Grove, PA). All other reagents were of analytical grade and were obtained from commercial sources.

### *Cell culture and differentiation*

Human myeloid THP-1 cells were grown in RPMI 1640 containing 10% FBS, 100 IU/ml of penicillin, 100 μg/ml of streptomycin, and 0.6 mg/ml of glutamine at 37°C in 95% air and 5% $CO_2$. THP-1 cells were caused to differentiate into neutrophil-like cells by treatment with 0.5 mM dibutyryl cAMP for 3 days.

### *Assay for in vitro Tyr kinase activity*

Lysates from the differentiated THP-1 cells were immunoprecipitated with various Abs specific for a certain type of Tyr kinases, and the in vitro Tyr kinase assay was performed with enolase as a substrate by the method described previously (12).

### *Immunoprecipitation and immunoblotting*

The differentiated THP-1 cells were washed with ice-cold PBS and a suspension buffer consisting of 10 mM HEPES-NaOH (pH 7.4), 136 mM NaCl, 4.9 mM KCl, 5.5 mM glucose, and 0.2% (w/v) BSA, and incubated in the suspension buffer containing 1 mM $CaCl_2$ at a density of ~$5 \times 10^7$ cells/ml. For stimulation of FcγRII, the cells ($1 \times 10^7$ cells/200 μl), after being held on ice for 25 min with 1 μg/ml of IV.3, were first incubated at 37°C for 5 min and further incubated for 2 min (or the indicated times) with 10 μg/ml of goat anti-mouse IgG (H + L) $F(ab')_2$ for the receptor cross-linking. In the indicated experiments, the cells were simultaneously stimulated with 1 μM fMLP at 37°C.

Tyr-phosphorylated proteins in the cells were analyzed, as described previously (5, 6). Briefly, the reaction was terminated by adding the same volume (200 μl) of a lysis buffer consisting of 40 mM HEPES-NaOH (pH 7.4), 150 mM NaCl, 30 mM NaF, 2 mM $Na_3VO_4$, 20 mM $Na_4P_2O_7$, 4 mM EDTA, 2% Nonidet P-40, and 10 μg/ml of aprotinin. The cell extract was immunoprecipitated with 1 μg of anti-p110β (or 4 μg of anti-Gab2/P or Gab2/C) and protein A-Sepharose resin. The precipitated proteins were subjected to SDS-PAGE (8% acrylamide), and the separated proteins were transferred onto a polyvinylidene difluoride membrane (Bio-Rad, Hercules, CA). In some experiments (see Fig. 4A), the immunocomplexes were diluted in a buffer consisting of 20 mM Tris-HCl (pH 7.4,) 50 mM NaCl, and

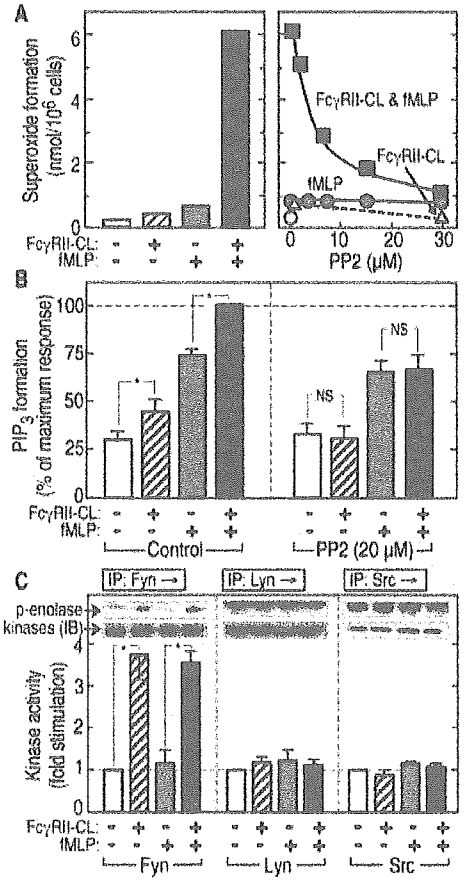


**FIGURE 1.** Enhancement of fMLP-induced superoxide formation by FcγRII cross-linking requires Tyr kinase-dependent $PIP_3$ formation in differentiated THP-1 cells. *A*, Differentiated THP-1 cells that had been treated with 1 μg/ml of the anti-FcγRII mAb (IV.3) were incubated at 37°C for 10 min (*A*) or 2 min (*B*) with 10 μg/ml of the goat anti-mouse IgG $F(ab')_2$ for cross-linking of the receptor (FcγRII-CL) in the presence and/or absence of 1 μM fMLP. The incubation mixture also contained 20 μM (*B*, *right columns*) or the indicated concentrations (*A*, *right panel*) of PP2. Superoxide formation (*A*) and $PIP_3$ production (*B*) in the cells were measured, as described in *Materials and Methods*. *C*, Lysates were prepared from the stimulated cells and immunoprecipitated with the indicated Abs specific for their Tyr kinases. In vitro Tyr kinase assay was performed, as described in *Materials and Methods*. The *insets* show $^{32}$P-phosphorylated enolase (*upper lanes*) and precipitated kinases (*lower lanes*) that were detected by their specific Abs. *Bars* indicate the SEs of means. Asterisks and NS indicate that the two paired values are statistically significant ($p < 0.05$) or not, respectively.

0.1% 2-ME, and incubated with 33 U of PP2A at 30°C for 30 min. The membrane, after being shaken in TBS (20 mM Tris-HCl, pH 7.5, and 150 mM NaCl) containing 5% BSA, was incubated with the indicated Abs at room temperature for 1 h and further incubated with $^{125}$I-labeled protein A or HRP-conjugated anti-rabbit IgG. The radioactivity and peroxidase activity retained on the membrane were visualized with a Fuji BAS 1800 and a LAS 1000 bioimaging analyzer (Fuji Film, Tokyo, Japan), respectively.

### *Preparation of recombinant proteins and affinity resin*

The aa sequence 312–725 of PI 3-kinase p85$\alpha$ subunit, which contains two SH2 domains, was produced in *Escherichia coli* as a GST-fused form and conjugated with activated Thiol-Sepharose 4B (Amersham Pharmacia Biotech, Piscataway, NJ), according to the manufacturer's instruction. THP-1 cells were stimulated, as described above, and the reaction was terminated by adding a buffer consisting of 4% SDS, 200 mM NaCl, 60 mM Tris-HCl (pH 7.4), 20 mM DTT, 5 mM $Na_3VO_4$, 8 $\mu$M leupeptin, and 0.8 $\mu$g/ml of pepstatin A. The cell extract was boiled for 5 min and treated with 30 mM *N*-ethylmaleimide. After 13-fold dilution with a buffer consisting of 1% Triton X-100, 80 mM NaCl, 30 mM Tris-HCl (pH 7.4), 0.5 mM $Na_3VO_4$, 5 $\mu$M leupeptin, and 0.5 $\mu$g/ml of pepstatin A, the cell extract was applied to the affinity resin. Proteins bound to the resin were eluted with a buffer consisting of 4% SDS, 1 mM EDTA, 1 mM $Na_3VO_4$, 10% glycerol, and 100 mM Tris-HCl (pH 6.8). Phosphorylation of the eluted proteins was visualized according to the method described above.

### *Transfection of Gab2 mutant*

The cDNA encoding a dominant-negative human Gab2 mutant (Y452/476/584F), whose Tyr residues contained in the putative p85-binding sites were all replaced by Phe, was constructed by Kunkel method. The Y-to-F mutant and wild-type Gab2 were cloned into mammalian expression vector pCMV5 and introduced into THP-1 cells by electroporation.

### *In vitro kinase and in-gel kinase assays*

COS7 cells were transfected with pcDNA3 vector encoding Flag-tagged Gab2 by electroporation. The Gab2 protein was immunoprecipitated with anti-Flag affinity gel (M2) and eluted with 1 mg/ml of Flag peptide. Active form of ERK2 was prepared from the differentiated THP-1 cells that had been stimulated with fMLP by immunoprecipitation using an anti-ERK2 Ab. The resultant resin containing the activated ERK2 was suspended in a kinase buffer consisting of 50 mM Tris-HCl (pH 7.5), 10 mM $MgCl_2$, 1 mM EGTA, 0.2 mM ATP, and 5 $\mu$Ci [$\gamma$-$^{32}$P]ATP. The solution was mixed with Flag-tagged Gab2 and incubated at 30°C for 30 min. Phosphorylated proteins were analyzed by SDS-PAGE (8% acrylamide), and the radioactivity was visualized with the bioimaging analyzer.

For *in-gel* kinase assay, the cell extract was separated by SDS-PAGE (10% acrylamide and 0.5 mg/ml of MBP), and SDS was removed by washing the gel twice with 125 ml of propanol solution (50 mM Tris-HCl, pH 8.0, and 20% 2-propanol) for 30 min. The gel, after being washed twice with 125 ml of buffer A (50 mM Tris-HCl, pH 8.0, and 5 mM 2-ME) for 30 min at room temperature, was denatured twice with 125 ml of buffer A containing 6 M guanidine hydrochloride for 30 min at room temperature and renatured with 100 ml of buffer A containing 0.04% (w/v) of Tween 40 for 16 h at 4°C. The gel was further washed twice with the same buffer for 30 min and incubated in buffer B (40 mM HEPES-NaOH, pH 7.5, 0.1 mM EGTA, 20 mM $MgCl_2$, and 2 mM DTT) for 1 h at 25°C. Phosphorylation of MBP was conducted by incubating the gel in buffer B containing 25 $\mu$M ATP and 2.5 $\mu$Ci/ml of [$\gamma$-$^{32}$P]ATP at 25°C for 1 h. After incubation, the gel was washed with a buffer consisting of 5% TCA and 1% sodium pyrophosphate. The radioactivity was visualized with the bioimaging analyzer.

### *Assays for superoxide formation and $PIP_3$ production in THP-1 cells*

Superoxide formation was determined by measuring the reduction of cytochrome *c*, as described previously (5). Briefly, the differentiated THP-1 cells were suspended in Hank's solution containing 10 mM HEPES-NaOH (pH 7.4), 1 mg/ml of BSA, and 1.2 mg/ml of cytochrome *c*. An aliquot (180 $\mu$l, $5 \times 10^6$ cells/ml) was first incubated at 37°C for 5 min with or without superoxide dismutase (170 U/ml) and further incubated with 20 $\mu$l of the indicated reagents at 37°C for the indicated times. The reaction was terminated by adding 10 $\mu$l of 40 mM *N*-ethylmaleimide, and the reduced cytochrome *c* was determined by spectroscopic analysis at 550 nm.

$PIP_3$ production was measured according to the method described by Okada et al. (9). The THP-1 cells were suspended at the density of $4 \times 10^7$ cells/ml in a labeling medium consisting of 10 mM HEPES-NaOH (pH 7.4), 136 mM NaCl, 4.9 mM KCl, and 5.5 mM glucose, and incubated at 37°C for 30 min with 500 $\mu$Ci/ml of $^{32}P_i$. The radiolabeled cells were washed twice with the same medium and resuspended at $5 \times 10^6$ cells/ml in the medium containing 1 mM $CaCl_2$. Aliquots (400 $\mu$l, $2 \times 10^6$ cells/ml) were preincubated for 5 min and further incubated with the indicated reagents. The reaction was terminated by the addition of 1.55 ml of chloroform/methanol/8% $HClO_4$ (50:100:5). Then 0.5 ml each of chloroform and 8% $HClO_4$ were added to the mixture, and the lipid phase was separated by centrifugation. The lipid phase was washed with chloroform-saturated 1 M NaCl containing 1% $HClO_4$ and dried. The extracted lipid was dissolved in 20 $\mu$l of chloroform/methanol (95:5) and spotted on a TLC plate (Silica gel 60; Merck, West Point, PA). Before spotting, the plate was once developed with methanol/water (2:3) containing 1.2% potassium oxalate and preactivated by heating at 110°C for 20 min. The plate was developed in chloroform/methanol/acetone/acetic acid/water (80:30:26:24:14), and radioactivities were visualized with the bioimaging analyzer.

## Results

### *Enhancement of fMLP-induced superoxide formation by FcγRII cross-linking requires Tyr kinase-dependent $PIP_3$ formation*

We first examined which subtypes of FcγRII were expressed in THP-1 cells by means of RT-PCR (data not shown). Nondifferentiated THP-1 cells contained both IIA and IIC types of FcγR. When the cells were differentiated into neutrophil-like cells by dibutyryl cAMP, there was a marked increase in the level of the type IIC receptor. However, neither nondifferentiated nor differentiated THP-1 cells contained the type IIB receptor. Thus, the neutrophil-like THP-1 cells used in the present study were revealed to possess only the ITAM-containing types of FcγR, IIA and IIC.

We previously showed that fMLP-induced superoxide formation was markedly enhanced by FcγRII stimulation in the differentiated THP-1 cells in a manner associated with the elevation of PI 3-kinase product $PIP_3$ (4–6). Moreover, the enhanced superoxide formation was completely abolished by treatment of the cells with the PI 3-kinase inhibitor wortmannin. These results indicate that FcγRII-dependent activation of the lipid kinase is involved in the cell response. We thus investigated the effect of PP2, a *Src*-type Tyr kinase inhibitor, on superoxide generation and $PIP_3$ formation in the neutrophil-like THP-1 cells. As shown in Fig. 1*A*, superoxide formation was synergistically stimulated by FcγRII cross-linking plus fMLP (*left columns*), and this response was progressively inhibited as the concentration of PP2 was increased (*right panel*). Similar inhibition was also observed in the cell response induced by Fcγ alone. However, the Tyr kinase inhibitor did not exert its influence on the action of fMLP alone. We also measured the intracellular accumulation of $PIP_3$ in the differentiated THP-1 cells under the same experimental conditions. There were further increases in $PIP_3$ formation upon the stimulation of FcγRII both in the presence and absence of fMLP (Fig. 1*B*, *left columns*). Interestingly, PP2 completely inhibited the action of FcγRII, but not the fMLP-induced $PIP_3$ formation (Fig. 1*B*, *right columns*).

We also examined which member of *Src*-type Tyr kinases is responsible for the FcγRII-dependent signaling in the cells. For the analysis, the cell lysates were immunoprecipitated with various Abs specific for a certain type of Tyr kinases and subjected to in vitro Tyr kinase assay with enolase as a substrate. As shown in Fig. 1*C*, *Fyn*, but not *Lyn* or *Src*, appeared to be activated by FcγRII cross-linking. We could not detect any activation of *Lck* or *Fgr*-type Tyr kinase (data not shown). These results suggest that PI 3-kinase is activated by FcγRII-linked *Fyn* Tyr kinase and that the lipid kinase activation is especially important for the synergistic superoxide formation observed with FcγRII cross-linking plus fMLP.

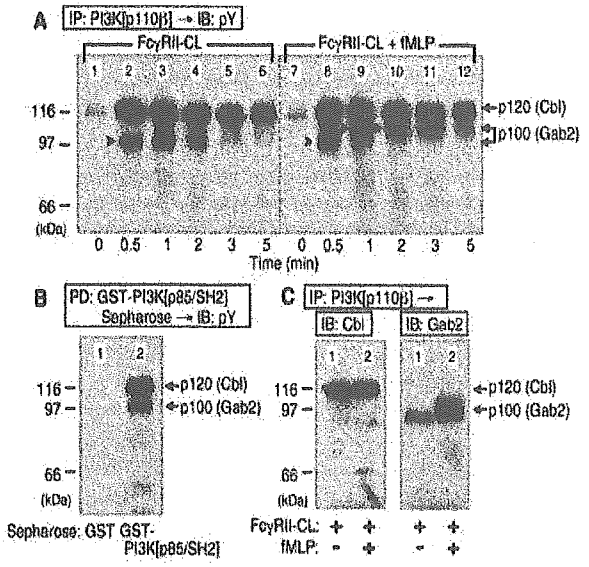


**FIGURE 2.** Stimulation of FcγRII induces Tyr phosphorylation of c-Cbl and Gab2 in differentiated THP-1 cells. The differentiated THP-1 cells were stimulated at 37°C for 2 min with FcγRII-CL and/or fMLP, as described in Fig. 1. *A*, The cell lysates were immunoprecipitated with an anti-p110β Ab, separated by SDS-PAGE, and subjected to immunoblot analysis with the anti-pY AB1600, as described in *Materials and Methods*. *B*, Proteins bound to the SH2 domains of p85 in the cell lysate (FcγRII-CL) were affinity purified by means of Sepharose resin conjugated with GST alone (*lane 1*) or GST-PI 3-kinase (p85/SH2) (*lane 2*), as described in *Materials and Methods*. *C*, The immunoblot analysis was performed with anti-Cbl (*left*) and anti-Gab2/C (*right*) Abs. The m.w. markers used were obtained from Bio-Rad and are indicated in kilodaltons.

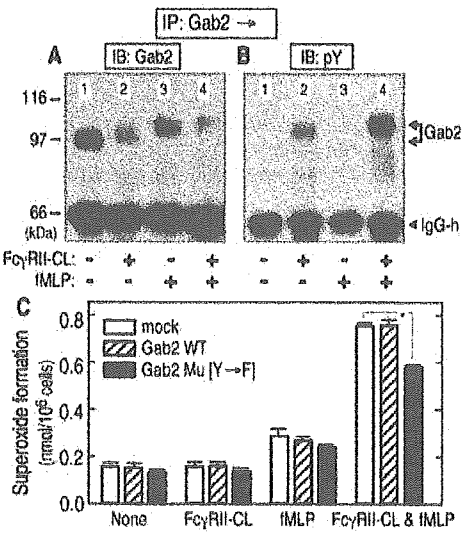


**FIGURE 3.** Stimulation of G protein-coupled fMLP receptor induces modification of the PI 3-kinase adaptor Gab2 that is responsible for the synergistic superoxide formation. The differentiated THP-1 cells were stimulated at 37°C for 2 min with FcγRII-CL and/or fMLP, as described in Fig. 1. The cell lysate was immunoprecipitated with anti-Gab2/P, separated by SDS-PAGE, and subjected to immunoblot analysis with anti-Gab2/C (*A*) and anti-pY AB1600 (*B*) Abs. *C*, THP-1 cells were transfected with wild-type Gab2 (WT) or its mutant (Mu) and caused to differentiation into the mid stage of neutrophil-like cells. Superoxide formation in response to FcγRII-CL and/or fMLP was measured, as described in *Materials and Methods*.

### *Identification of PI 3-kinase adaptors in FcγRII-stimulated THP-1 cells*

To understand the molecular mechanism of this synergistic activation, we next investigated Tyr-phosphorylated proteins associated with the class I p110β/p85 PI 3-kinase. The differentiated THP-1 cells were stimulated with FcγRII cross-linking, and PI 3-kinase-associated proteins were immunoprecipitated with an Ab raised against the p110β catalytic subunit. The precipitated proteins were separated by SDS-PAGE and immunoblotted with an anti-phospho-Tyr Ab. As shown in Fig. 2*A* (*lanes 1–6*), 120-kDa (p120) and 100-kDa (p100) proteins were Tyr phosphorylated in the FcγRII-stimulated cells. When the cells were simultaneously stimulated with fMLP (Fig. 2*A*, *lanes 7–12*), a time-dependent mobility shift of p100 was clearly observed without a significant change in the profile of p120. We further examined whether the Tyr-phosphorylated proteins were capable of interacting with PI 3-kinase through SH2 domains of p85 using affinity resin conjugated with GST-fused p85α SH2 (the aa sequence 312–725). As shown in Fig. 2*B* (*lane 2*), both the Tyr-phosphorylated p120 and p100 were capable of binding to the SH2 domains. Based on their molecular weights and immunoreactivity, p120 and p100 could be identified as c-Cbl and Gab2, respectively (Fig. 2*C*). These results indicate that p120/c-Cbl and p100/Gab2 function as adaptor molecules for the p110/p85 PI 3-kinase in the FcγRII-stimulated THP-1 cells.

### *Modification of the PI 3-kinase adaptor Gab2 by fMLP receptor stimulation*

Because the PI 3-kinase adaptor Gab2 displayed its unique properties upon fMLP receptor stimulation, we further investigated the properties of Gab2 in the differentiated THP-1 cells. The cells stimulated with FcγRII and/or fMLP receptors were lysed and immunoprecipitated with the anti-Gab2/P, and the precipitated proteins were analyzed by immunoblot using anti-Gab2/C and anti-phospho-Tyr (AB1600) Abs. As shown in Fig. 3, stimulation by FcγRII induced slightly, but significantly the mobility shift (*A*, *lane 2*) and Tyr phosphorylation (*B*, *lane 2*) of Gab2. In contrast, stimulation by fMLP induced more apparent mobility shift (*A*, *lane 3*), but no Tyr phosphorylation (*B*, *lane 3*) of Gab2. Costimulation with FcγRII and fMLP receptors enhanced the mobility shift (*A*, *lane 4*) and Tyr phosphorylation (*B*, *lane 4*) of Gab2. As expected, the p85-regulatory and the p110β-catalytic subunits of PI 3-kinase could be more immunoprecipitated with Gab2 when Tyr phosphorylation of the adaptor was further enhanced by costimulation with fMLP (data not shown). Furthermore, Gab2-associated PI 3-kinase activity observed upon FcγRII cross-linking was certainly enhanced by the costimulation. These results indicate that fMLP induces certain modification of Gab2 in a manner different from FcγRII-induced Tyr phosphorylation, and that this modification is responsible for the enhanced PI 3-kinase activity.

The contribution of Tyr phosphorylation of the PI 3-kinase adaptor Gab2 to superoxide formation was partly confirmed by transfection experiments with a dominant-negative Gab2 mutant (Y452/476/584F), whose putative Tyr residues contained in the binding sites for p85 were all replaced by Phe. For this analysis, THP-1 cells were transiently transfected with the Gab2 mutant (or its wild type) and caused to differentiate into the mid stage of neutrophil-like cells by 1-day culture, because further incubation inhibited the protein expression, and because the prior transfection reduced the differentiation. Although the cell differentiation and transfection efficiency (~50%) were limited under the present conditions, superoxide formation in response to FcγRII cross-linking plus fMLP was significantly attenuated in the Gab2 mutant-transfected cells in comparison with mock- or wild-type Gab2-transfected cells (Fig. 3*C*). Thus, the PI 3-kinase adaptor Gab2 appeared

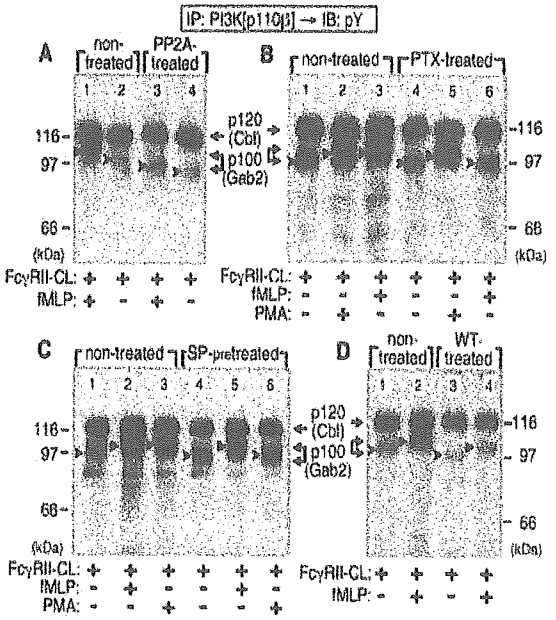


**FIGURE 4.** Characterization of the fMLP-induced modification of the PI 3-kinase adaptor Gab2. The differentiated THP-1 cells were stimulated at 37°C for 2 min with FcγRII-CL and/or fMLP, as described in Fig. 1, and the cell lysates were immunoprecipitated with anti-p110β Ab, separated by SDS-PAGE, and subjected to immunoblot analysis with anti-pY AB1600 Ab. *A*, The immunoprecipitated samples were incubated at 30°C for 30 min with (*lanes 3* and *4*) or without (*lanes 1* and *2*) 33 U of PP2A before the immunoblot analysis. *B–D*, the THP-1 cells were pretreated at 37°C with 50 ng/ml of pertussis toxin (*PTX*) for 4 h (*B*, *lanes 4–6*), 5 μM staurosporine (*SP*) for 10 min (*C*, *lanes 4–6*), or 1 μM wortmannin (*WT*) for 10 min (*D*, *lanes 3* and *4*), before the cell stimulation with FcγRII-CL, fMLP, and/or 0.5 μM PMA.

to be responsible, if not all, for the synergistic superoxide formation induced by the two different types of receptors.

### *Ser/Thr phosphorylation of the PI 3-kinase adaptor Gab2 by G protein-coupled fMLP receptor stimulation*

To reveal the entity of the fMLP-induced modification of Gab2, the adaptor protein that had been immunoprecipitated with anti-p110β Ab was treated with a protein phosphatase (PP2A) specific for Ser/Thr phosphorylation. As shown in Fig. 4*A*, PP2A treatment altered the mobility shift of Tyr-phosphorylated Gab2 induced by fMLP (compare *lanes 1* and *3*). Furthermore, PP2A changed the mobility shift of Tyr-phosphorylated Gab2 induced by FcγRII stimulation (*lanes 2* and *4*). These results suggest that Gab2 is phosphorylated at Ser/Thr residues by the stimulation of fMLP receptors and FcγRII, in addition to its Tyr phosphorylation by FcγRII.

We next examined how fMLP receptor-dependent signaling pathways are related to the Ser/Thr phosphorylation of Gab2. Pertussis toxin, which inhibits the coupling of fMLP receptor to $G_i$-type G proteins, was first used for the analysis. Differentiated THP-1 cells that had been treated with pertussis toxin were stimulated with Fcγ and/or fMLP, and the cell lysate was immunoprecipitated with anti-p110β and immunoblotted with anti-phospho-Tyr (AB1600) Abs (Fig. 4*B*). The fMLP-induced mobility shift of Gab2 was almost completely abolished after the toxin treatment (compare *lanes 3* and *6*), indicating that activation of $G_i$ is required for the Gab2 phosphorylation.

To identify the Ser/Thr kinase(s) involved in the fMLP-induced Gab2 phosphorylation, we examined effects of a protein kinase C activator (PMA) and a kinase inhibitor (staurosporine). Similar to the fMLP stimulation, PMA induced mobility shift of Gab2 (Fig. 4, *B*, *lane 2*, and *C*, *lane 3*), although this PMA-induced mobility shift was insensitive to pertussis toxin (Fig. 4*B*, *lane 5*). As expected, staurosporine inhibited the PMA-induced mobility shift of Gab2 (Fig. 4*C*, *lane 6*). However, the kinase C inhibitor failed to inhibit the action of fMLP (Fig. 4*C*, *lane 5*). These results indicate that neither protein kinase C nor a staurosporine-sensitive kinase(s) is involved in the fMLP-induced Ser/Thr phosphorylation of Gab2.

A recent report showed that another Ser/Thr kinase, protein kinase B, which is activated by the PI 3-kinase product $PIP_3$, phosphorylates Gab2 at Ser 159 and negatively regulates heregulin-induced mitogenic signaling (13). In the report, heregulin-induced Tyr phosphorylation of Gab2 is enhanced by pretreatment with the specific PI 3-kinase inhibitor wortmannin. Therefore, we examined effect of wortmannin on the mobility shift of Gab2. There was decrease in the level of Tyr-phosphorylated Gab2 in cells treated with wortmannin (Fig. 4*D*, *lanes 3* and *4*). Furthermore, the action of fMLP was still clearly observed under the conditions that PI 3-kinase was inhibited by wortmannin. These results indicate that PI 3-kinase-dependent kinases including protein kinase B are not responsible for the fMLP-induced Ser/Thr phosphorylation of Gab2.

### *Involvement of ERK in the fMLP-induced Ser/Thr phosphorylation of Gab2*

A recent report showed that Gab1, which is a member of Gab family, is phosphorylated, possibly at $Thr^{476}$, by ERK after hepatocyte growth factor stimulation (14). Because Gab2 has a corresponding amino acid $Ser^{491}$ to the $Thr^{476}$ of Gab1, we examined whether ERK activation may be involved in the fMLP-induced Ser/Thr phosphorylation of Gab2. Differentiated THP-1 cells that had been treated with an ERK kinase (mitogen-activated protein kinase kinase) inhibitor, PD98059, were stimulated with FcγRII cross-linking and fMLP, and the cell lysate was immunoprecipitated and immunoblotted by anti-Gab2 Ab. Interestingly, PD98059 significantly inhibited the fMLP-induced mobility shift of Gab2 (Fig. 5*A*, *lanes 7* and *8*). We next examined ERK activity by an in-gel kinase assay. Lysate prepared from the stimulated THP-1 cells was applied on SDS polyacrylamide gel containing the ERK substrate MBP, and in-gel phosphorylation was performed in the presence of [$\gamma$-$^{32}$P]ATP. As shown in Fig. 5*B* (*lanes 3* and *4*), there were phosphorylated bands at the positions of 42 kDa (ERK1) and 40 kDa (ERK2) upon the cell stimulation with fMLP. The fMLP-dependent activation of ERK1 and ERK2 was progressively inhibited as the concentration of PD98059 was increased (Fig. 5*C*). We also examined whether activated ERK in the fMLP-stimulated cells is capable of phosphorylating Gab2 in vitro using a recombinant Flag-tagged Gab2. As shown in Fig. 5*D*, recombinant Flag-tagged Gab2 was clearly phosphorylated by the activated ERK obtained from the fMLP-treated cells.

### *Inhibition of the Ser/Thr phosphorylation of PI 3-kinase adaptor Gab2 affects superoxide formation and $PIP_3$ production*

We finally investigated whether the Ser/Thr phosphorylation of PI 3-kinase adaptor Gab2 exerts its influence on the lipid kinase activity and superoxide formation in the differentiated THP-1 cells. As shown in Fig. 6*A*, enhanced superoxide formation stimulated by FcγRII cross-linking plus fMLP was inhibited significantly, but partially by PD98059 under the conditions that the ERK-dependent Ser/Thr phosphorylation of Gab2 was profoundly suppressed (see Fig. 5). It is worth noting that PD98059 did not affect superoxide formation induced by either FcγRII cross-linking or fMLP.

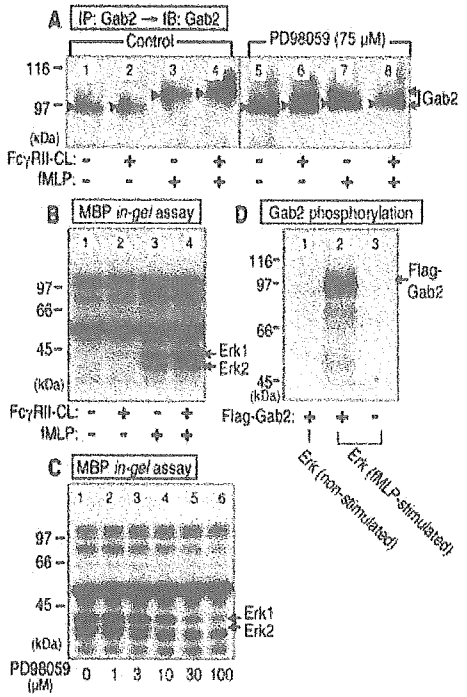


**FIGURE 5.** fMLP-induced Ser/Thr phosphorylation of Gab2 is mediated through activation of ERK. The differentiated THP-1 cells were stimulated at 37°C for 2 min with FcγRII-CL and/or fMLP, as described in Fig. 1, in the presence or absence of 75 μM PD98059. *A*, The cell lysate was immunoprecipitated with anti-Gab2/C Ab and subjected to immunoblot analysis with the same Ab. *B* and *C*, The cell lysates were subjected to an in-gel kinase assay with MBP, as described in *Materials and Methods*. Various concentrations of PD98059 were used in the stimulation of THP-1 cells with FcγRII-CL and fMLP (*C*). *D*, An in vitro kinase assay was performed with a recombinant Flag-tagged Gab2 (*lanes 1* and *2*), as described in *Materials and Methods*. The cell lysate containing ERK was prepared from the cells that had been stimulated with fMLP (*lanes 2* and *3*) or not (*lane 1*).

Interestingly, PD98059 also abolished the enhanced $PIP_3$ formation induced by Fcγ plus fMLP without significant changing in the stimulatory action of fMLP or FcγRII cross-linking alone (Fig. 6*B*, *right columns*). These effects induced by the ERK inhibition were quite different from those observed with PP2 (see Fig. 1). Thus, the synergistic superoxide formation appeared to be mediated through the Tyr kinase-linked signaling pathway, which possibly involves the modification of PI 3-kinase adaptor Gab2 found in the present study. The partial inhibition observed with PD98059 suggests that there is another mechanism in the synergistic superoxide formation by the two different types of membrane receptors (see *Discussion*).

## Discussion

We previously searched for various intracellular messengers that may be responsible for fMLP-induced superoxide formation in differentiated THP-1 cells and found that the activation of PI 3-kinase plays an important role in the cell function (4, 5). Interestingly, intracellular formation of $PIP_3$ was significantly enhanced by the costimulation of FcγRII and fMLP receptors in THP-1 cells (5, 6). Furthermore, we established that the class Ia PI 3-kinase p110β/p85 could be synergistically activated by a Tyr-phosphorylated peptide and βγ subunits of G proteins (10) and showed that a specific PI 3-kinase inhibitor, wortmannin, completely inhibited the superoxide formation (5). However, it remained to be determined how p110β/p85 is synergistically activated in intact cells. Our present study focusing on its adaptor molecules basically ex-

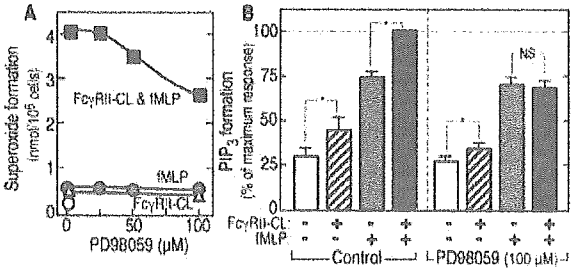


**FIGURE 6.** Effects of PD98059 on superoxide formation and PI 3-kinase activity. The differentiated THP-1 cells were stimulated at 37°C for 10 min (*A*) or 2 min (*B*) with FcγRII-CL and/or fMLP, as described in Fig. 1. The incubation mixture also contained 100 μM (*B*) or the indicated concentrations of PD98059 (*A*). Superoxide formation (*A*) and $PIP_3$ production (*B*) in the stimulated THP-1 cells were measured, as described in *Materials and Methods*. *B*, Bars indicate the SEs of means. Asterisks and NS indicate that the two paired values are statistically significant ($p < 0.05$) or not, respectively.

tends the above molecular mechanism and indicates a novel pathway leading to efficient PI 3-kinase activation. The new findings obtained in this study are summarized in Fig. 7.

First, we identified Gab2 and c-Cbl as adaptor molecules for the class Ia PI 3-kinase in the FcγRII-stimulated cells, because both proteins were Tyr phosphorylated and associated with the lipid kinase through SH2 domains of p85 (see Fig. 2). Second, the adaptor Gab2 was rapidly modified by $G_i$-coupled fMLP receptor stimulation in terms of its mobility shift on SDS-PAGE (see Fig. 4). Moreover, the mobility shift of Gab2 occurred without Tyr phosphorylation on the adaptor molecule. The entity of the Gab2 modification was proven to be phosphorylation at Ser/Thr residue(s), and $G_i$-dependent ERK activation appeared to be responsible for the Ser/Thr phosphorylation (see Figs. 4 and 5). Indeed, activated ERK obtained from fMLP-stimulated THP-1 cells directly phosphorylated Gab2 (see Fig. 5*D*). Although similar modification of

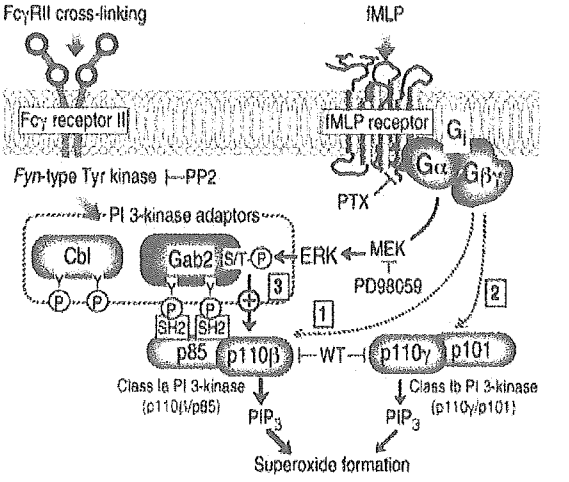


**FIGURE 7.** A schematic representation of signal transduction pathways involved in FcγRII- and fMLP receptor-induced $PIP_3$ production and superoxide formation. Superoxide formation by the stimulation of FcγRII and fMLP receptors involves various signal transduction pathways, including: 1) the synergistic activation of p110β/p85-type PI 3-kinase by the stimulation through p85/SH2 domains and p110β by the adaptors and G protein βγ subunits, respectively (10); 2) the activation of p110γ/p101-type PI 3-kinase by G protein βγ subunits (11); and 3) the activation of Gab2-associated PI 3-kinase through the Ser/Thr phosphorylation of the adaptor observed in the present study. See *Discussion* section for further explanation.

Gab2 was observed with PMA in a manner sensitive to staurosporine (see Fig. 4, *B* and *C*), neither protein kinase C nor protein kinase B was involved in the fMLP-induced Ser/Thr phosphorylation of Gab2.

Gab2 belongs to Daughter OF SevenLes (DOS)/Gab family scaffolding adaptors that contain N-terminal pleckstrin homology domain and multiple Tyr residues, which serve as binding sites upon phosphorylation for many signal-relay molecules, including Grb2, SHP-2, and p85 of PI 3-kinase (13, 15–19), as confirmed in the present study. In addition to the Tyr phosphorylation sites, DOS/Gab family possesses many Ser/Thr phosphorylation sites for a number of protein kinases. Ser/Thr phosphorylation, as well as Tyr phosphorylation after receptor stimulation, is commonly used to regulate the adaptor function both positively and negatively (13, 14, 20–24). In this study, we found that Ser/Thr residue(s) of Gab2 was phosphorylated by $G_i$-coupled fMLP receptor stimulation and that ERK is involved in the Ser/Thr phosphorylation. Indeed, Gab2 has five Pro-X-(X)-Ser/Thr-Pro sequences that can be phosphorylated by ERK. The $Ser^{491}$ within Pro-Met-Ser-Pro sequence on Gab2 may be phosphorylated by ERK, because another member of Gab family, Gab1, is phosphorylated at $Thr^{476}$ within Pro-Met-Thr-Pro corresponding to the sequence of Gab2 (14). In addition, it is very likely that fMLP induces modification of Gab2 other than the ERK-dependent phosphorylation, because there was still significant difference in the mobility shift of Gab2 between the presence and absence of fMLP even after PP2A treatment (see Fig. 4*A*, *lanes 3* and *4*).

We have previously reported that stimulation of two different types of membrane receptors induces synergistic activation of PI 3-kinase, which leads to enhanced cell functions (5, 9, 25). The activation of $G_i$ through the stimulation of G protein-coupled membrane receptors appears to be responsible for the enhanced $PIP_3$ formation and cell functions possibly through the following three different mechanisms. The first one is dependent on the unique properties of class Ia PI 3-kinase consisting of p110$\beta$ and p85. The heterodimeric PI 3-kinase could be synergistically activated by a Tyr-phosphorylated peptide and $\beta\gamma$ subunits resolved from $G_i$ (9) (see Fig. 7, *route 1*). The target site of the $\beta\gamma$ subunit-dependent activation is present in p110$\beta$-catalytic subunit of PI 3-kinase rather than its regulatory p85 subunit, because other PI 3-kinase subtypes, p110$\alpha$/p85 and p110$\delta$/p85, were insensitive to the $\beta\gamma$ subunits (10, 11). Second, $\beta\gamma$ subunits of G protein are also capable of activating the p110$\gamma$/p101-type PI 3-kinase (10, 11) (see Fig. 7, *route 2*). The p110$\gamma$-catalytic subunit is a site for the stimulatory action of the $\beta\gamma$ subunits, and p101 appears to be responsible for the substrate selectivity of the p110$\gamma$ type for PI-4, 5-bisphosphate (11). It has recently been reported that neutrophil functions induced by G protein-coupled receptors, such as fMLP-induced cell migration and respiratory burst, are severely impaired in mice lacking p110$\gamma$ (26–28). Thus, p110$\gamma$ PI 3-kinase appears to be a major subtype responsible for the neutrophil functions.

In addition to the above two mechanisms, we found in this study that dual-phosphorylated form of Gab2 may also serve as a cross talk molecule between the two distinct signals (see Fig. 7, *route 3*). The small, but significant enhancement of $PIP_3$ formation, which was sensitive to the inhibition of Gab2 Ser/Thr phosphorylation by PD98059, appeared to be partly involved in the potentiation of superoxide formation (see Fig. 6). Thus, $PIP_3$ formation at a locally targeting site within the cells may lead to the effective superoxide formation. It is well known that neutrophil functions are potentiated when the cells are also primed with inflammatory cytokines before fMLP stimulation (29–33). Among them, GM-CSF, which linked to tyrosine kinase activities, enhanced $PIP_3$ and superoxide generation, which were both sensitive to wortmannin (31) and severely impaired in p85$\alpha$ knockout mice (33). Interestingly, PD98059 inhibited partially the enhanced superoxide formation in GM-CSF-primed human neutrophils (31). Therefore, in certain situations, the novel pathway revealed in this study may play an important physiological role in effective host defense in intact cells.

## References


1. Luster, A. D. 1998. Chemokines: chemotactic cytokines that mediate inflammation. *N. Engl. J. Med. 338:436.*
2. Panaro, M. A., and V. Mitolo. 1999. Cellular responses to FMLP challenging: a mini-review. *Immunopharmacol. Immunotoxicol. 21:397.*
3. Mansour, M. K., and S. M. Levitz. 2002. Interactions of fungi with phagocytes. *Curr. Opin. Microbiol. 5:359.*
4. Okada, T., L. Sakuma, Y. Fukui, O. Hazeki, and M. Ui. 1994. Blockage of chemotactic peptide-induced stimulation of neutrophils by wortmannin as a result of selective inhibition of phosphatidylinositol 3-kinase. *J. Biol. Chem. 269:3563.*
5. Tsujimoto, N., K. Kontani, S. Inoue, S. Hoshino, O. Hazeki, F. Malavasi, and T. Katada. 1997. Potentiation of chemotactic peptide-induced superoxide generation by CD38 ligation in human myeloid cell lines. *J. Biochem. 121:949.*
6. Inoue, S., K. Kontani, N. Tsujimoto, Y. Kanda, N. Hosoda, S. Hoshino, O. Hazeki, and T. Katada. 1997. Protein-tyrosine phosphorylation by IgG1 subclass CD38 monoclonal antibodies is mediated through stimulation of the Fc$\gamma$II receptors in human myeloid cell lines. *J. Immunol. 159:5226.*
7. Vanhaesebroeck, B., and M. D. Waterfield. 1999. Signaling by distinct classes of phosphoinositide 3-kinases. *Exp. Cell Res. 253:239.*
8. Sotsios, Y., and S. G. Ward. 2000. Phosphoinositide 3-kinase: a key biochemical signal for cell migration in response to chemokines. *Immunol. Rev. 177:217.*
9. Okada, T., O. Hazeki, M. Ui, and T. Katada. 1996. Synergistic activation of PtdIns 3-kinase by tyrosine-phosphorylated peptide and $\beta\gamma$-subunits of GTP-binding proteins. *Biochem. J. 317:475.*
10. Kurosu, H., T. Maehama, T. Okada, T. Yamamoto, S. Hoshino, Y. Fukui, M. Ui, O. Hazeki, and T. Katada. 1997. Heterodimeric phosphoinositide 3-kinase consisting of p85 and p110$\beta$ is synergistically activated by the $\beta\gamma$ subunits of G proteins and phosphotyrosyl peptide. *J. Biol. Chem. 272:24252.*
11. Maier, U., A. Babich, and B. Nurnberg. 1999. Roles of non-catalytic subunits in G$\beta\gamma$-induced activation of class I phosphoinositide 3-kinase isoforms $\beta$ and $\gamma$. *J. Biol. Chem. 274:29311.*
12. Kitagawa, D., S. Tanemura, S. Ohata, N. Shimizu, J. Seo, G. Nishitai, T. Watanabe, K. Nakagawa, H. Kishimoto, T. Wada, et al. 2002. Activation of extracellular signal-regulated kinase by ultraviolet is mediated through Src-dependent epidermal growth factor receptor phosphorylation: its implication in an anti-apoptotic function. *J. Biol. Chem. 277:366.*
13. Lynch, D. K., and R. J. Daly. 2002. PKB-mediated negative feedback tightly regulates mitogenic signalling via Gab2. *EMBO J. 21:72.*
14. Yu, C. F., B. Roshan, Z. X. Liu, and L. G. Cantley. 2001. ERK regulates the hepatocyte growth factor-mediated interaction of Gab1 and the phosphatidylinositol 3-kinase. *J. Biol. Chem. 276:32552.*
15. Gu, H., J. C. Pratt, S. J. Burakoff, and B. G. Neel. 1998. Cloning of p97/Gab2, the major SHP2-binding protein in hematopoietic cells, reveals a novel pathway for cytokine-induced gene activation. *Mol. Cell 2:729.*
16. Zhao, C., D. H. Yu, R. Shen, and G. S. Feng. 1999. Gab2, a new pleckstrin homology domain-containing adapter protein, acts to uncouple signaling from ERK kinase to Elk-1. *J. Biol. Chem. 274:19649.*
17. Nishida, K., Y. Yoshida, M. Itoh, T. Fukada, T. Ohtani, T. Shirogane, T. Atsumi, M. Takahashi-Tezuka, K. Ishihara, M. Hibi, and T. Hirano. 1999. Gab-family adapter proteins act downstream of cytokine and growth factor receptors and T- and B-cell antigen receptors. *Blood 93:1809.*
18. Gadina, M., C. Sudarshan, R. Visconti, Y. J. Zhou, H. Gu, B. G. Neel, and J. J. O'Shea. 2000. The docking molecule gab2 is induced by lymphocyte activation and is involved in signaling by interleukin-2 and interleukin-15 but not other common $\gamma$ chain-using cytokines. *J. Biol. Chem. 275:26959.*
19. Yamasaki, S., K. Nishida, M. Sakuma, D. Berry, C. J. McGlade, T. Hirano, and T. Saito. 2003. Gads/Grb2-mediated association with LAT is critical for the inhibitory function of Gab2 in T cells. *Mol. Cell. Biol. 23:2515.*
20. Roshan, B., C. Kjelsberg, K. Spokes, A. Eldred, C. S. Crovello, and L. G. Cantley. 1999. Activated ERK2 interacts with and phosphorylates the docking protein GAB1. *J. Biol. Chem. 274:36362.*
21. Paz, K., Y. F. Liu, H. Shorer, R. Hemi, D. LeRoith, M. Quan, H. Kanety, R. Seger, and Y. Zick. 1999. Phosphorylation of insulin receptor substrate-1 (IRS-1) by protein kinase B positively regulates IRS-1 function. *J. Biol. Chem. 274:28816.*
22. Aguirre, V., T. Uchida, L. Yenush, R. Davis, and M. F. White. 2000. The c-Jun NH(2)-terminal kinase promotes insulin resistance during association with insulin receptor substrate-1 and phosphorylation of Ser(307). *J. Biol. Chem. 275:9047.*
23. Migliaccio, E., M. Giorgio, S. Mele, G. Pelicci, P. Reboldi, P. P. Pandolfi, L. Lanfrancone, and P. G. Pelicci. 1999. The p66shc adaptor protein controls oxidative stress response and life span in mammals. *Nature 402:309.*
24. Voisin, L., L. Larose, and S. Meloche. 1999. Angiotensin II stimulates serine phosphorylation of the adaptor protein Nck: physical association with the serine/threonine kinases Pak1 and casein kinase I. *Biochem. J. 341:217.*
25. Takasuga, S., T. Katada, M. Ui, and O. Hazeki. 1999. Enhancement by adenosine of insulin-induced activation of phosphoinositide 3-kinase and protein kinase B in rat adipocytes. *J. Biol. Chem. 274:19545.*

26. Sasaki, T., J. Irie-Sasaki, R. G. Jones, A. J. Oliveira-dos-Santos, W. L. Stanford, B. Bolon, A. Wakeham, A. Itie, D. Bouchard, I. Kozieradzki, et al. 2000. Function of PI3Kγ in thymocyte development, T cell activation, and neutrophil migration. *Science 287:1040.*

27. Li, Z., H. Jiang, W. Xie, Z. Zhang, A. V. Smrcka, and D. Wu. 2000. Roles of PLC-β2 and -β3 and PI3Kγ in chemoattractant-mediated signal transduction. *Science 287:1046.*

28. Hirsch, E., V. L. Katanaev, C. Garlanda, O. Azzolino, L. Pirola, L. Silengo, S. Sozzani, A. Mantovani, F. Altruda, and M. P. Wymann. 2000. Central role for G protein-coupled phosphoinositide 3-kinase γ in inflammation. *Science 287:1049.*

29. Sullivan, G. W., H. T. Carper, and G. L. Mandell. 1993. The effect of three human recombinant hematopoietic growth factors (granulocyte-macrophage colony-stimulating factor, granulocyte colony-stimulating factor, and interleukin-3) on phagocyte oxidative activity. *Blood 81:1863.*

30. Condliffe, A. M., P. T. Hawkins, L. R. Stephens, C. Haslett, and E. R. Chilvers. 1998. Priming of human neutrophil superoxide generation by tumor necrosis factor-α is signalled by enhanced phosphatidylinositol 3, 4, 5-trisphosphate but not inositol 1, 4, 5-trisphosphate accumulation. *FEBS Lett. 439:147.*

31. Kodama, T., K. Hazeki, O. Hazeki, T. Okada, and M. Ui. 1999. Enhancement of chemotactic peptide-induced activation of phosphoinositide 3-kinase by granulocyte-macrophage colony-stimulating factor and its relation to the cytokine-mediated priming of neutrophil superoxide-anion production. *Biochem. J. 337:201.*

32. Cadwallader, K. A., A. M. Condliffe, A. McGregor, T. R. Walker, J. F. White, L. R. Stephens, and E. R. Chilvers. 2002. Regulation of phosphatidylinositol 3-kinase activity and phosphatidylinositol 3, 4, 5-trisphosphate accumulation by neutrophil priming agents. *J. Immunol. 169:3336.*

33. Yasui, K., Y. Sekiguchi, M. Ichikawa, H. Nagumo, T. Yamazaki, A. Komiyama, and H. Suzuki. 2002. Granulocyte macrophage-colony stimulating factor delays neutrophil apoptosis and primes its function through Ia-type phosphoinositide 3-kinase. *J. Leukocyte Biol. 72:1020.*

# Weak agonist self-peptides promote selection and tuning of virus-specific T cells

**Samuel D. Saibil[1], Toshiaki Ohteki[1], Forest M. White[2], Mark Luscher[3], Arsen Zakarian[1], Alisha Elford[1], Jeffery Shabanowitz[2], Hiroshi Nishina[1], Patrice Hugo[4], Josef Penninger[1], Brian Barber[3], Donald F. Hunt[2] and Pamela S. Ohashi[1]**

[1] University Health Network, Ontario Cancer Institute, Departments of Medical Biophysics and Immunology, Toronto, Canada
[2] Department of Chemistry, University of Virginia, Charlottesville, USA
[3] Department of Medicine, University of Toronto, Toronto, Canada
[4] Procrea BioSciences, Montreal, Canada

Recent progress has begun to define the interactions and signaling pathways that are triggered during positive selection. To identify and further examine self-peptides that can mediate positive selection, we searched a protein-database to find peptides that have minimal homology with the viral peptide (p33) that activates a defined P14 transgenic TCR. We identified four peptides that could bind the restriction element H-2D$^b$ and induce proliferation of P14 transgenic splenocytes at high concentration. Two of the four peptides (DBM and RPP) were able to positively select the virus-specific TCR in fetal thymic organ culture but were unable to induce clonal deletion. Reverse-phase HPLC and mass spectrometry demonstrated that these peptides were presented by H-2D$^b$ molecules on thymic epithelial cell lines. We also examined whether the selecting ligands altered T cell responsiveness *in vitro*. DBM-selected T cells lost their ability to respond to the positively selecting ligand DBM, whereas RPP-selected T cells only retained their ability to respond to high concentrations of RPP. These results demonstrate that self-peptides that mediate positive selection can differentially "tune" the activation threshold of T cells and alter the functional repertoire of T cells.

| | |
|---|---|
| Received | 13/5/02 |
| Revised | 17/12/02 |
| Accepted | 15/1/03 |

**Key words:** Positive selection / Self-peptide / T cell activation thresholds / Tuning

## 1 Introduction

The diversity of TCR that is found in the periphery represents the confluence of two opposing, yet complementary, thymic processes: positive and negative selection. Within the thymus, cells bearing TCR that are capable of recognizing self-peptide–MHC complexes within a prescribed window of affinity/avidity are positively selected to survive, mature and emigrate. T cells with TCR that react too strongly (i.e. with too much affinity/avidity) to these same self-peptide–MHC complexes are induced to die by the process of negative selection (selection is reviewed in reference [1]). Negative selection is one important mechanism that prevents autoimmunity as it limits the escape of self-reactive T cells into the periphery. Conversely, positive selection is responsible for the survival of useful MHC-restricted T cells.

Within this model of T cell selection, the self-peptide–MHC complexes found in the thymus play a role in shaping the TCR repertoire as they mediate both selection processes. The nature of these self-peptide complexes has been the focus of several studies. Collectively, these studies provide strong evidence that positive selection can be mediated by ubiquitously expressed self-peptides that contain no significant homology to the cognate peptide of the selected TCR [2–6]. If T cells are indeed selected on ubiquitously expressed self-peptides, then the potential for self-reactivity in the periphery exists. The question remains as to the mechanisms of tolerance that prevent the activation of these cells and the development of autoimmunity.

Grossman and colleagues [7–9] developed the "tunable activation thresholds" (TAT) hypothesis to explain how T cells avoid becoming inappropriately activated by self-peptide. The TAT hypothesis posits that T cell activation

[I 23143]

The first two authors contributed equally to this manuscript.

**Abbreviations: β2m:** β2 Microglobulin **DP:** Double-positive **FTOC:** Fetal thymic organ culture **LCMV:** Lymphocytic choriomeningitis virus **SP:** Single-positive



0014-2980/03/0303-685$17.50+.50/0